Commensurate melting, domain walls, and dislocations

David A. Huse
*AT&T Bell Laboratories, Murray Hill, New Jersey 07974**
and Baker Laboratory, Cornell University, Ithaca, New York 14853

Michael E. Fisher
Baker Laboratory, Cornell University, Ithaca, New York 14853
(Received 18 April 1983)

Commensurate phases of order $p \geq 3$ exhibit two or more classes of inequivalent domain walls, reflecting a lower than ideal symmetry. These walls compete statistically and undergo wetting transitions. New "chiral" universality classes of melting transitions may thereby occur for both 3×1 and $\sqrt{3}\times\sqrt{3}$ surface phases. The data of Moncton *et al.* may be interpreted as indicating that such a chiral transition occurs in Kr on graphite. The melting of $p\times1$ phases is discussed for various dimensionalities d and values of p. Domain-wall wetting transitions are treated in a semiphenomenological fashion; they may be either continuous or first order. Wetting critical exponents are obtained for a general class of transitions. The role of dislocations at the uniaxial commensurate-to-incommensurate transition is examined. For $d=2$ the crossover exponent for dislocations is found to be $-\theta_p=(6-p^2)/4$. For $p>\sqrt{6}$ the dislocations are therefore irrelevant, but they introduce singular corrections to scaling at the transition. A phase diagram as a function of dislocation fugacity is proposed for the case $d=2$, $p=3$, illustrating how a Lifshitz point may be present at all nonzero fugacities.

I. INTRODUCTION AND SUMMARY

Consider a physical system in which one set of degrees of freedom are spatially ordered and form an essentially rigid, infinite, periodic lattice, although the full translational symmetry of this *underlying lattice* may be broken by some other set or sets of degrees of freedom. In the typical case, the first set of degrees of freedom are represented by the positions of a set of atoms or ions which provide the "bulk framework" of the system. The other degrees of freedom, whose ordering transitions are the focus of interest, might be realized by superimposed displacements of mass, by the positions of another set of particles, or by charge or spin and magnetization densities. The corresponding ordered phases are then represented by standing waves of mass, composition, charge, or spin density that form a superlattice within a bulk crystal, a "reconstructed" surface of the crystal, or an adsorbed phase on the surface, etc. The resulting superlattice may be either *commensurate* with the underlying lattice or *incommensurate.* The simplest situation conceptually, and the one whose language we will adopt even though many of the ideas and results are general, is that of a submonolayer or near monolayer of atoms adsorbed on a surface which presents a regular array—the underlying lattice—of adsorption sites.

As one varies the temperature, chemical potential, or other thermodynamic fields, an ordered, solidlike *commensurate phase* may *melt* either into a disordered fluidlike phase (a "gas") or via a commensurate-to-incommensurate transition, into a "floating solidlike" *incommensurate phase.* It is found, particularly in two-dimensional or surface systems, that both types of melting may occur as continuous (i.e., critical) phase transitions, in contrast to the traditional first-order melting of a bulk three-dimensional crystal lattice. Both types of transition are presently of appreciable experimental and theoretical interest, the nature of the possible continuous transitions being a central issue. The physical system in which such phase transitions have been most thoroughly studied is Kr on graphite.[1–6] Other experimental systems in which commensurate melting has been investigated include He on graphite,[7] O on Ni(111),[8] Xe on Cu (110),[9] N_2 on graphite,[10] and, in bulk systems, thiourea[11] and bromine-intercalated graphite.[12] Theoretical models which have been devised and studied include the Frenkel-Kontorowa model,[13] the sine-Gordon model,[14–16] the axial next-nearest-neighbor Ising (ANNNI) model,[17–21] the chiral clock models,[22–28] and various lattice gases.[29–32]

Domany *et al.*[33] have classified various two-dimensional fluid-to-commensurate phase transitions into universality classes on the basis of symmetry rules due to Landau and Lifshitz and renormalization-group ideas. They suggest, for example, in agreement with previous work of Alexander,[34] that the order-disorder transition of the so-called $\sqrt{3}\times\sqrt{3}R30°$ commensurate phase on a triangular array of substrate sites, such as provided by the ideal surface of graphite, should be a continuous transition in the three-state Potts-model universality class. This prediction has been confirmed experimentally by Bretz,[7] who observed the divergence of the specific heat of He on graphite at or close to the ideal coverage, and obtained a critical exponent, α, consistent with the accepted three-state, two-dimensional Potts value,[35,36] $\alpha=\frac{1}{3}$. Equally, this prediction is confirmed by Baxter's exact solution of the so-called "hard hexagon" model, i.e., a triangular lattice gas

with infinite nearest-neighbor repulsions.[29]

However, it has been pointed out[6,37] that the symmetry of a gas adsorbed on a substrate presenting a surface of triangular lattice character is, in fact, generally lower than that of an ideal Potts model. Further, the present authors have argued that such lower symmetry may lead to new types of phase transitions, which, indeed, might already have been observed.[37] Thus, high-resolution measurements of synchroton x rays scattered from Kr on graphite[4] have revealed a transition from a fluid phase to a $\sqrt{3}\times\sqrt{3}R30°$ commensurate solid phase that does *not* appear to belong to the universality class of three-state Potts models.[37] The lower symmetries of such adsorbed gas systems correspond to Potts or clock models with additional symmetry-breaking terms that couple the abstract discrete spin space (of Potts variables) to real space. A principal aim of the present paper is to explore the consequences of such a lower symmetry for both $\sqrt{3}\times\sqrt{3}$ and $p\times 1$ phases in physical systems and in model systems. The first few sections constitute mainly an expanded and, we hope, more transparent exposition of the ideas presented in Ref. 37. The role of dislocations at uniaxial commensurate-to-incommensurate phase transitions in two dimensions is then investigated. For the convenience of the reader we summarize our work briefly here.

The fact that the overall physical symmetry of an adsorbate forming a $p\times 1$ commensurate phase on a substrate is lower than that of a simple p-state clock model is made apparent in Sec. II by examining the interfaces or domain walls separating distinct domains of the commensurate phase. The nature of such an interface parallel to a given direction and hence its free energy or interfacial tension, Σ, is found to depend on the orientational *sense* defined by the two domains it separates: Thus, in contrast to the situation in the usual discrete spin models, an $A\,|\,B$ wall (parallel, say, to the y axis) may have a different tension than the corresponding $B\,|\,A$ wall. The simplest models embodying this feature, and thus appropriate for modeling $p\times 1$ commensurate phases, are the *chiral clock models,*[22,23] which contain couplings between the discrete abstract spin space and real space. To understand the effect on the melting transition of breaking the full Potts or clock symmetry in this chiral fashion, the first question we ask is whether or not the chiral symmetry breaking constitutes a *relevant operator* (in the usual renormalization group sense) at the symmetric or "pure clock" critical point. For the p-state ($p\geq 3$) chiral clock models we find that the chiral field is always relevant and causes crossover to phase transitions which belong to different universality classes than those of the symmetric clock models. The resulting phase diagrams[22,38,39] for the chiral clock models are discussed for various dimensionalities, d, and state numbers, p. For $p=3$ and $d=2$ a new class of *chiral* order-disorder phase transitions is indicated,[37] we expect that a continuous melting transition of 3×1 commensurate surface phase will in general be in this new universality class, whose properties are discussed in Sec. IV. (Implicitly we assume here and below that the continuous melting transition is not preempted by some extrinsic first-order transition). Haldane *et al.*[15] and Schulz[16] have suggested that 3×1 commensurate phases will not melt directly into a disordered fluid, except at points of special symmetry; rather, they argue that an intermediate incommensurate phase should appear. This would imply that the chiral transition does not occur for $p=3$, $d=2$. However, their arguments are strictly valid only in a limit in which the density of dislocations in the adsorbate layer vanishes, and so have no convincing applicability to systems at typical melting temperatures, where there are many dislocations present. Furthermore, some numerical work on the two-dimensional three-state chiral clock model does suggest that there are direct commensurate-to-disordered phase transitions over a range of parameters for $p=3$.[25,27]

The chiral symmetry breaking operator appropriate for systems that form a $\sqrt{3}\times\sqrt{3}R30°$ commensurate phase is of a different (triaxial) form than that introduced in the (uniaxially) chiral clock models. When expressed in terms of a Landau-Ginzburg-Wilson Hamiltonian, it is of third order in the gradient of the order parameter and therefore appears to be irrelevant at the symmetric critical point. This irrelevance is confirmed by the exact solution of the hard hexagon model,[29,40,41] which exhibits a melting transition in the *symmetric* Potts-model universality class even though triaxially chiral symmetry breaking is present in the model. However, we interpret (in Sec. IV) the experimental evidence for Kr on graphite[4] as indicating that this and other triaxially chiral symmetry breaking operators can, if present in sufficient strength, cause crossover from simple three-state Potts melting to "triaxial" chiral melting. A plausible phase diagram for Kr on graphite, proposed in Sec. IV,[37] contains a new multicritical point where this crossover occurs.

The crossover scaling exponent, ϕ_p, of the chiral field at the symmetric critical point of a uniaxially chiral clock model may be calculated analytically for various values of p and d.[38,39] These exact results are discussed in Sec. III; all are consistent with a formula, based on scaling arguments supplemented by plausible assumptions, which relates ϕ_p to the exponents μ_p and β_p for the interfacial tension and order parameter, respectively, of the symmetric model. For the experimentally interesting case $p=3$ and $d=2$ this formula, namely, $\phi_p=\mu_p-2\beta_p$, yields $\phi_3=11/18\simeq 0.61$ [if one accepts the conjectured values of μ_p and β_p for the ($p=3$)-state Potts model].[35,36] However, direct numerical estimation based on high- and low-temperature series expansions for the $d=2,p=3$ chiral clock model[28] suggests $\phi_3=0.19\pm 0.06$. This value, while still indicating that the chiral perturbation *is relevant,* clearly casts doubt on the generality of the theoretical assumptions made; in addition its surprisingly small magnitude probably means that it will be rather difficult to detect the chiral crossover to new critical behavior in simulations[25] or in experimental systems.

As is explained above and expounded in detail in Sec. II, the interfaces between different domains of a commensurate phase will, for $p\geq 3$, have different interfacial tensions, depending on their orientational sense. When the interfacial tension, or excess free energy per unit length, of one type of wall becomes large enough relative to others, the wall will become unstable and split into two (or more) separate walls of another type while a layer (or

layers) of one (or more) further domain(s) intrude between the two domains that the wall originally separated. Such interfacial *wetting transitions*[28,37] change the nature of the dominant fluctuations near the chiral melting line, thus playing an important role in the crossover from ordinary Potts or clock to specifically chiral critical behavior, as is discussed in Sec. VI.

The phenomenological analysis of the uniaxial commensurate-incommensurate transition in d dimensions presented by Fisher and Fisher[42] is extended in Sec. VII to obtain scaling forms for the free energy and susceptibility near the transition. The role of *dislocations* at this transition is then examined, particularly for two dimensions. We obtain, in Sec. VIII, a dislocation-dislocation correlation function in the commensurate phase of the two-dimensional system and postulate a scaling form that contains both our result and that of Schulz, Halperin, and Henley,[43] who have calculated the same correlation function in the incommensurate phase for distances large compared to the correlation length. By integrating this correlation function to obtain a susceptibility, we find that the crossover scaling exponent for the dislocation fugacity is $\frac{1}{4}(6-p^2)$. For $p=2$ this means that the dislocations are relevant; they cause crossover to an Ising transition as was shown by Bohr.[44] For the less than realistic cases $\sqrt{6}<p<\sqrt{8}$ the dislocations are irrelevant at the commensurate-incommensurate *transition*, but are relevant *in* the incommensurate phase, which therefore melts into a fluid.[5,19,22] For $p>\sqrt{8}$, the dislocations are always irrelevant, but they do give rise to critical singularities on the commensurate side of the transition that are not present when dislocations are forbidden and which might be observable.

In the last section we examine the role of dislocations in the two-dimensional chiral clock model, particularly for $p=3$. A microscopic location may be assigned to each dislocation core in a configuration of the chiral clock model. Each dislocation core sits within a plaquette so the core energy may simply be introduced as a controllable parameter in the model by adding plaquette (i.e., multispin) interactions to the Hamiltonian. The expected phase diagram for such a three-state chiral clock model illustrates how the Lifshitz multicritical point and new chiral melting transition, which are not present when dislocations are forbidden, may appear as the dislocation fugacity is increased from zero.

II. DOMAIN WALLS AND SYMMETRY

Our analysis addresses systems where, in the commensurate phase, the full translational symmetry of an underlying lattice is spontaneously broken. As mentioned above, a variety of different physical systems exhibit such phases but we will use the language appropriate to commensurate ordering of adsorbed atoms on a regular lattice of adsorption sites; nevertheless, the basic ideas apply quite generally.

In the simple commensurate phases that we will consider, one of $p=2,3,\ldots,$ equivalent but distinct sublattices, $A,B,C,\ldots,$ of adsorption sites is preferentially occupied by the adatoms. One may also consider phases in which more than one sublattice is preferentially occupied or where one has molecular adsorbates with orientational degrees of freedom, but only the simpler case is addressed explicitly here. In the fluid or melted phase the various sublattices are, statistically, all equally occupied. The sublattice structure exhibits an abstract *internal symmetry* represented, say, by a group Y_p, whose elements permute the different sublattices. In particular, we will focus attention on $p\times 1$ commensurate phases, where an absorbate on a *rectangular* substrate forms an overlayer with an x-axis lattice constant p times that of the array of adsorption sites, and on $\sqrt{3}\times\sqrt{3}R30°$ commensurate phases on a triangular array of adsorption sites with *hexagonal* symmetry such as occurs in He or Kr on graphite. The ground states of two 3×1 phases and the $\sqrt{3}\times\sqrt{3}R30°$ phase are illustrated in Fig. 1. Dissociated hydrogen on Fe(110) forms a 3×1 phase ordered as in Fig. 1(b), with the large spots representing *un*occupied adsorption sites, or holes.[45]

At the fluid-to-commensurate transition the sublattice symmetry, Y_p, is spontaneously broken. One might then expect that the phase transition is in the same universality class as the standard Ising, Potts, or clock-model phase transition where the corresponding "spin" symmetry is broken.[33,46] Of course, the symmetry may also be broken via a first-order phase transition, such as occurs for Kr on graphite at low chemical potential or vapor pressure.[1,2] Indeed one must anticipate that atoms with sufficiently attractive interactions will always condense via a first-order transition at low pressures. However, we focus here on the possible types of *continuous* phase transitions that might occur at higher pressures and coverages.

A continuous transition to a $p=2$ commensurate phase, where one of two equivalent sublattices is selected, should be in the Ising universality class.[33] For $p=2$ this simple assignment of universality class appears to be quite generally valid. On the other hand, in the next simplest case,

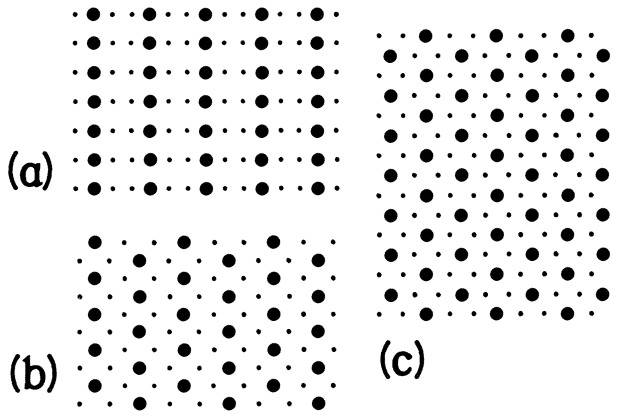

FIG. 1. Idealized representation of simple commensurate adsorbed phases of order $p=3$. The dots represent the adsorption sites of the underlying, substrate lattice while the closed circles depict structureless adsorbate particles. Parts (a) and (b) illustrate simple rectangular and centered rectangular 3×1 phases, respectively, while (c) represents a hexagonal $\sqrt{3}\times\sqrt{3}R30°$ phase as found in He and Kr on graphite. Dissociated hydrogen on Fe(110) displays a phase ordered as in (b) but with two sublattices occupied and one vacant (see Ref. 45).

$p=3$, where one might expect the continuous melting transition to always be in the three-state Potts universality class,[33,34] we will conclude, as explained below, that *new* types of continuous phase transitions may occur. Similar conclusions apply for larger p.

The universality class of a phase transition in a given system is determined to a large degree by the symmetry and dimensionality of the system. The simple p-state Potts or clock models have a symmetry that is the direct product of the internal spin symmetry Y_p and the independent lattice symmetry, say L. However, the adatom-substrate system has a smaller symmetry group, say G, that is only a subgroup of $Y_p \times L$. The origin of this lower symmetry may be demonstrated in an instructive manner by examining *walls* or *interfaces* separating different domains of the ordered phase.[6,37] There are p distinct types of ordered domains: Let us label these by the corresponding sublattice, $A,B,C,\ldots$, that the adatoms in the domain preferentially occupy. A domain wall *oriented in a particular direction* may, in general, be one of $p(p-1)$ types, depending on which domains it separates. Thus for $p=3$ and walls parallel to, say, the y axis we have domain walls of the types $A \mid B$, $B \mid C$, $C \mid A$, $A \mid C$, $C \mid B$, and $B \mid A$. The full $S_3 \times L$ symmetry of a three-state Potts or clock model dictates that these walls are all equivalent to one another so that they all have *identical* excess free energies per unit length or interfacial tensions, $\Sigma_0(T)$.

On the other hand, for 3×1 rectangular or $\sqrt{3}\times\sqrt{3}$ hexagonal commensurate phases the $A \mid B$ and $B \mid A$ domain walls are *intrinsically different,* even when oriented parallel to the same direction.[6,37] This is illustrated in Fig. 2 for a rectangular phase and in Fig. 3 for a hexagonal phase. Note that these figures are *schematic* with neglect of any displacements of the adsorbed particles from the ideal adsorption sites (as well as neglect of any vacancies or interstitials). With regard to the order-disorder phenomena, such displacements may reasonably be ignored well inside a commensurate domain, but they must play an important role in the vicinity of a domain wall where, in fact, they determine the microscopic *width* of the wall.[47] However, the idealization used in Figs. 2 and 3 suffices to reveal clearly the intrinsically distinct structures of parallel $A \mid B$ and $B \mid A$ walls.

It is also evident for the 3×1 rectangular and hexagonal phases illustrated that the sublattice symmetries dictate that the $A \mid B$, $B \mid C$, and $C \mid A$ walls oriented in a given direction are all equivalent to one another; we will call them $[+]$ walls. The three remaining types of wall are likewise equivalent and will be called $[-]$ walls. It would seem from the figures, however, that the two types of wall can occur naturally either in a "heavy" form, as illustrated on the left sides of Figs. 2 and 3, or in a "light" form as shown on the right sides. In the idealized heavy walls presented in the figures the $[+]$ and $[-]$ interfaces are denser than the ideal, commensurate surface coverage of $\theta_0=\frac{1}{3}$ particles per adsorption site, by an amount which corresponds to a net *adsorption* on the wall of two-thirds and one-third of a row of particles, respectively. Conversely, the ideal light $[+]$ and $[-]$ walls are less dense, having *negative* adsorptions (or deficits) of one-third and two-thirds of a row, respectively. It is clear physically that an "overpressure" (or excess chemical potential) which increases the coverage, θ, significantly above the commensurate value $\theta_0=\frac{1}{3}$, will tend to favor heavy walls; on the other hand an "underpressure," and corresponding lower than ideal coverage, will normally favor light walls. It is important to realize, however, that the adsorptions quoted are ideal values that represent, at best, bounds on the actual adsorptions. Thus as the chemical potential, say ζ, increases at constant T and the mean coverage in the commensurate phase changes from significantly below θ_0 to above θ_0, the adsorption on, say, a $[+]$ wall, should increase continuously from a negative value,

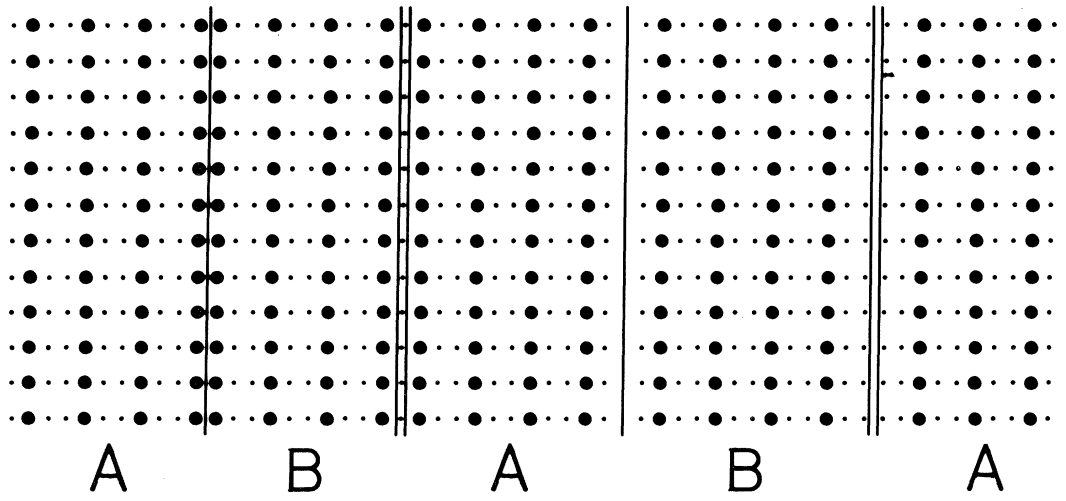

FIG. 2. Schematic depiction of $A \mid B$ and $B \mid A$ walls in a 3×1 rectangular phase. The idealized walls on the left are heavy while the topologically equivalent ideal walls on the right are light. At given temperature, T, and chemical potential, ζ, in a realistic situation all walls would, statistically, display misplaced particles, vacancies, and interstitials resulting in the same mean structure for all $A \mid B$ interfaces and for all $B \mid A$ interfaces: However, the $A \mid B$ and $B \mid A$ structures would remain distinct.

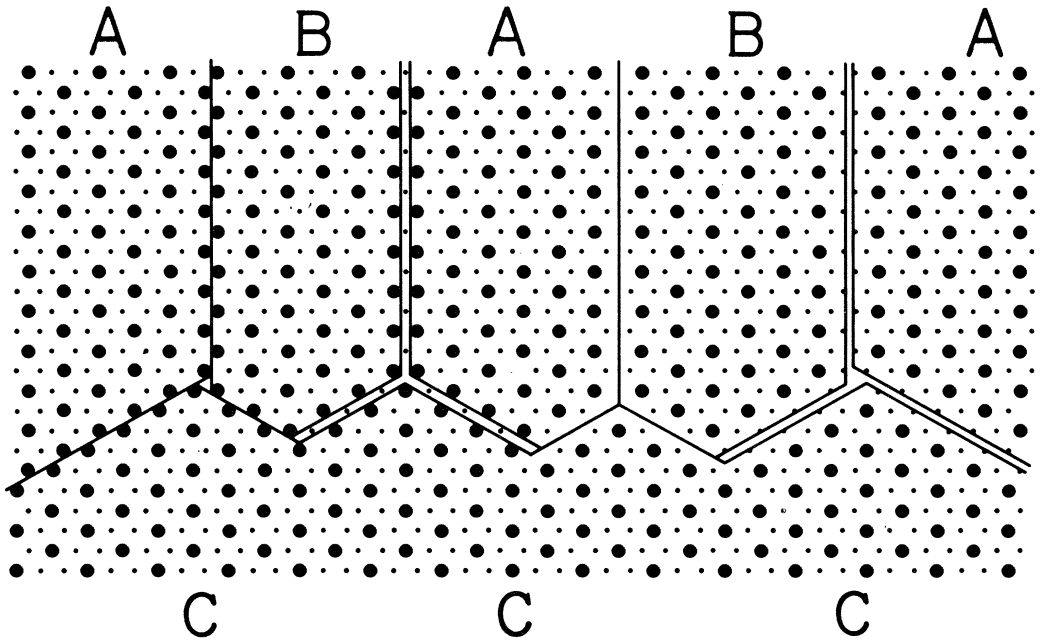

FIG. 3. Illustration of domain walls in a hexagonal $\sqrt{3}\times\sqrt{3}R30°$ commensurate phase illustrating two distinct types of wall in their idealized heavy form on the left and the corresponding idealized light form on the right. Note how the character of the $A \mid C$ and $B \mid C$ walls changes as the walls alter their directions. Junctions of three walls also arise in just two distinct forms represented here by the domain configurations (ACB) and (BCA).

probably greater than $-\frac{1}{3}$, to a positive value, perhaps approaching $+\frac{2}{3}$. The absorption on a $[-]$ wall should likewise increase continuously. The mechanism for this is, of course, simply the appearance in the interface of a statistical distribution, depending on T and ζ, of vacancies, interstitials, and particles on "wrong" absorption sites.

It remains true, nevertheless, that at any point the microscopic structures of $[+]$ and $[-]$ walls will differ. Consequently, the two types of wall will have *distinct* interfacial tensions, $\Sigma_+(T,\zeta)$ and $\Sigma_-(T,\zeta)$ which, in general, will be unequal. It may happen that over the accessible range of the commensurate phase one tension will always be smaller than the other; but if this is not so there should exist a locus within the commensurate phase, say $\zeta_0(T)$, on which the wall tensions are equal, i.e., $\Sigma_+=\Sigma_-$. The previous heuristic arguments suggest that this is likely to correspond to coverages, θ, near $\theta_0=\frac{1}{3}$; however, the details of the interatomic potentials, etc., might change this. Be that as it may, the adsorptions on a $[+]$ and $[-]$ wall can be related to the variation of $\Sigma_+(T,\zeta)$ and $\Sigma_-(T,\zeta)$, since by standard thermodynamic reasoning[48] one sees that they are simply proportional to the derivatives $-(\partial\Sigma_+/\partial\zeta)_T$ and $-(\partial\Sigma_-/\partial\zeta)_T$, respectively. Thus when ζ rises above $\zeta_0(T)$ the wall with the greater adsorption, i.e., the heavy wall, will be the one with lower interfacial tension. *A priori* one cannot be certain that the $[+]$ wall will be the "heavier" one since as demonstrated in Figs. 2 and 3, both types of wall may actually have either a positive or a negative adsorption. In fact it is not impossible for the two walls to interchange roles, there being two (or even more) distinct chemical potential values at which the equality $\Sigma_+=\Sigma_-$ is realized for a given temperature. However, this seems unlikely to occur in practice; rather we expect that there will normally be only a single locus, $\zeta_0(T)$, within the commensurate phase region of the (T,ζ) plane on which the wall tensions are equal. The wall with the greater adsorbate density *at* $\zeta_0(T)$ will then be the favored, low-tension wall for all $\zeta>\zeta_0(T)$. One must be cautious, however, in calling this wall the "heavy wall" because, in general, it will not remain the heavier wall in terms of the adsorption. On the contrary, since *both* tensions will vanish, and hence again become equal, on any portions of the phase boundary where the melting is continuous, the adsorption on the unfavored, originally lighter wall must increase and exceed that on the favored wall.

While there are just two types of domain wall for the simple $p=3$ systems, there will, in general be $p-1$ inequivalent types of wall for $p\times1$ rectangular phases, with interfacial tensions, say, $\Sigma_{+1},\Sigma_{+2},\ldots,\Sigma_q\equiv\Sigma_{-(p-q)}$ corresponding to $A \mid B$, $A \mid C$, $A \mid D$, ..., walls, etc. Thus for commensurate phases of order $p=2$ there is only one type of domain wall and it seems fairly certain that the simple Ising or Z_2 symmetry suffices for a correct description. However, for $p\geq3$ the existence of $p-1$ inequivalent types of domain wall demonstrates unequivocally that adsorbate systems have a *lower* symmetry than the standard p-state Potts or p-state clock models. For the three-state Potts model, for example, the internal $Y_3=S_3$ spin symmetry and the lattice symmetry, L, are clearly uncoupled. On the other hand the labels A, B, and C in a $p=3$ commensurate adatom-substrate system do *not* simply represent the values of an abstract discrete or Potts spin variable, say $n=0,1,2$; rather they represent sublattices in real space. Thus in a general commensurate phase of or-

der p, the internal symmetry, Y_p, and the lattice symmetry, L, are not independent; instead the full symmetry group G is a subgroup of $Y_p \times L$.

Now if we neglect translations, the $p=3$ rectangular lattice system illustrated in Fig. 2 has a symmetry group of twelve elements. Six consist of the three cyclic or even permutations of the sublattice labels, A, B, and C, combined with the two symmetry operations of the lattice that preserve the orientation of the x axis, namely the identity and a reflection about the x axis. The other six elements consist of the three antisymmetric or odd permutations of the sublattice labels combined with the two symmetry operations of the lattice that reverse the x axis. The simplest discrete spin model that embodies precisely this symmetry is the *three-state chiral clock model,*[22,23] which should therefore be appropriate for modeling the continuous melting of a 3×1 commensurate phase.[22,37]

The general p-state chiral clock model[22] consists of Potts or clock spin variables, n_i, situated at the sites, i, of a regular lattice. Each spin variable may assume one of the p values $n_i=0,1,\ldots,(p-1)$. In the simplest version of this model,[22] which should nevertheless be adequate for modeling the melting of $p\times 1$ phases, these spins are coupled by the Hamiltonian

$$\mathscr{H}=-J\sum_{\langle i,j\rangle}\cos[2\pi(n_i-n_j+\vec{\Delta}\cdot\vec{\mathrm{R}}_{ij})/p]\ , \tag{2.1}$$

where the sum runs over all nearest-neighbor pairs of sites and $\vec{\mathrm{R}}_{ij}$ is the vector from site i to site j. (Of course, one can allow the couplings, J, to be anisotropic in real space, but this will not affect the qualitative phase-transition behavior.) When the chiral field, $\vec{\Delta}$, vanishes, this model reduces to the standard clock model,[49] in which the Z_p spin and spatial symmetries are independent. The chiral field, $\vec{\Delta}$, which discriminates energetically between, for example, the linearly adjacent spin configurations 012 and 210, couples the abstract Potts spin space to real space, thereby lowering the overall symmetry of the model. Varying the chiral field clearly corresponds to varying the chemical potential in the adsorbate system; the arguments presented above lead to the identification

$$|\vec{\Delta}|\sim\zeta-\zeta_0(T)\ . \tag{2.2}$$

The chiral field here effectively couples to a *uniaxially chiral symmetry breaking operator* that selects a particular direction in space, namely, the orientation of the vector $\vec{\Delta}$. The consequences of including such an operator in the p-state clock model are examined in the next few sections.

The underlying triangular lattice in a $\sqrt{3}\times\sqrt{3}R30°$ ordered commensurate phase has a higher symmetry than a rectangular lattice, and so a different, *triaxially chiral Potts model* is appropriate for modeling the melting of such phases. The simplest triaxially chiral three-state Potts model is defined on a triangular lattice with plaquette interactions coupling the three spins around each elementary triangle. There are four possible plaquette energies in this model: one for plaquettes with all three spins in the same state, which indicates the three spins belong to the same microdomain; one for plaquettes with all three spins in different states that therefore represent a junction of three microdomain walls (such as occurs in Fig. 3); and two for plaquettes with two spins in one state and one spin in another state. This last type of plaquette is evidently crossed by a microdomain wall and its energy should thus depend on the wall type. An explicit representation of this triaxially chiral Potts model is the following: Let the spin at each site, j, of the triangular lattice have the three possible (complex) values $\psi_j=1$, $\exp(\pm 2\pi i/3)$. If the (horizontal) x axis is parallel to a nearest-neighbor direction then each elementary triangular plaquette may clearly be classified as pointing either upwards or downwards; let $\epsilon_{ijk}=+1$ if the plaquette comprised of sites i, j, and k points upwards, while $\epsilon_{ijk}=-1$ otherwise. Then the Hamiltonian is

$$\mathscr{H}=-J\sum_{\langle i,j\rangle}\mathrm{Re}(\psi_i^*\psi_j)+\sum_{(i,j,k)}[J_3\mathrm{Re}(\psi_i\psi_j\psi_k)+\Delta\epsilon_{ijk}\mathrm{Im}(\psi_i\psi_j\psi_k)]\ , \tag{2.3}$$

where the sums run over all nearest-neighbor pairs of sites and all elementary plaquettes, respectively.

Kardar and Berker[6] have introduced a rather similar model for modeling Kr on graphite. They observed the role of two types of domain wall (heavy and "superheavy") but in their detailed treatment each spin is intended to represent an entire domain, whose size is an additional parameter in the model. Their basic spin Hamiltonian differs from that introduced here in having only one possible energy for each segment of microdomain wall, while having two different energies for wall junctions. The energetics of the large heterodomain fluctuations that must play an important role in any continuous melting transition are determined to leading order by the energies of the associated microdomain walls. The energetics of wall *junctions* presumably plays only a secondary role. Thus in order to study the effects of triaxially chiral symmetry breaking on continuous three-state Potts model melting, the coupling of the chiral operator to microdomain-wall energies should be included explicitly in the model Hamiltonian, as in (2.3). This model and the symmetries of $\sqrt{3}\times\sqrt{3}R30°$ and other commensurate phases will be discussed in more detail in future work. However, some of the consequences of triaxially chiral symmetry breaking are discussed below.

III. THE CHIRAL CROSSOVER EXPONENT FOR GENERAL DIMENSIONALITY

The first question to ask about the consequences of chiral symmetry breaking is whether or not the chiral field $\vec{\Delta}$ is relevant, in the standard renormalization-group sense, at the symmetric Potts or clock critical points. To study this we consider the scaling properties in the vicinity of the symmetric critical point, $T=T_c^0$ and $\vec{\Delta}=0$, of the p-state chiral clock model (2.1) in d spatial dimensions (afterwards focusing on the case $d=2$ and $p=3$ of particular interest to us). Thus as the reduced temperature deviation,

$$t=(T-T_c^0)/T_c^0\ , \tag{3.1}$$

and the chiral field become small, the free energy per site,

$f(T,\vec{\Delta})$, and other thermodynamic quantities such as the surface tension, $\Sigma_{+1}(T,\vec{\Delta})$, of an $A\,|\,B$ wall should be governed, asymptotically, by scaling functions of the argument $\vec{y}=\vec{\Delta}/|t|^{\phi}$, where ϕ is the *chiral crossover exponent*.[39,50] If ϕ is positive the chiral field is *relevant* and we expect crossover to new, characteristically chiral critical behavior for $\vec{\Delta}\neq 0$; conversely, if ϕ is negative the chirality is *irrelevant* and, at least for small enough values of $\vec{\Delta}$, we expect no change in the nature of the transition which should then remain in the pure Potts ($p\leq 3$) or symmetric clock universality class. Thus for the singular part of the free energy above T_c and for the surface tension we anticipate[28,39]

$$f_s(T,\vec{\Delta})\approx t^{2-\alpha}W(\Delta/t^{\phi})\,, \tag{3.2}$$

$$\Sigma_{+1}(T,\vec{\Delta})\approx |t|^{\mu}S(\Delta/|t|^{\phi})\,, \tag{3.3}$$

where $\Delta=|\vec{\Delta}|$ and α and μ are the specific-heat and surface-tension exponents at $\Delta=0$; for convenience we suppose that the chiral field lies parallel to a symmetry axis, say the x axis, which is normal to the interface. By differentiating with respect to Δ we obtain

$$\chi_{\Delta\Delta}(T,\Delta=0)=\left[\frac{\partial^2 f}{\partial\Delta^2}\right]_{\Delta=0}\sim t^{2-\alpha-2\phi} \tag{3.4}$$

and

$$\left[\frac{\partial\Sigma_{+1}}{\partial\Delta}\right]_{\Delta=0}\sim |t|^{\mu-\phi}\,. \tag{3.5}$$

From these expressions we see that ϕ may be determined by studying properties of the symmetric model. [Note, however, that we implicitly assume that the appropriate scaling functions, (d^2W/dy^2) and (dS/dy), do not vanish identically when the argument $y=\Delta/|t|^{\phi}$ approaches zero, in which case the corrections to scaling would dominate.]

A. Four-state chiral clock model

The simplest case to consider[39] is $p=4$ since the correspondence

$$\sigma_i=\sqrt{2}\cos[\tfrac{1}{2}\pi(n_i+\tfrac{1}{2})],\quad \tau_i=\sqrt{2}\sin[\tfrac{1}{2}\pi(n_i+\tfrac{1}{2})] \tag{3.6}$$

shows that the pure, $\vec{\Delta}=0$ clock model with Hamiltonian (2.1) is equivalent to two *uncoupled* Ising models with spins $\sigma_i,\tau_i=\pm 1$. By noticing that the chiral operator for small Δ is then proportional to $\sigma_i\tau_{i'}-\tau_i\sigma_{i'}$, where i and i' denote neighboring spins along the chiral axis, one can readily evaluate the chiral susceptibility $\chi_{\Delta\Delta}$ at $\Delta=0$ in terms of Ising-model correlation functions $\langle\sigma_i\sigma_j\rangle$ and $\langle\tau_i\tau_j\rangle$. Knowing the scaling behavior of the Ising correlation functions enables one[39] to evaluate the divergence of $\chi_{\Delta\Delta}$ and from (3.4) one then concludes, quite generally, that the crossover exponent is given by

$$\phi_4=\gamma_4-\nu_4\,. \tag{3.7}$$

The subscripts here serve as a reminder that $p=4$, while the γ and ν denote, as usual, the exponents of divergence of the susceptibility and correlation length in terms of the standard, *longitudinal* correlation functions

$$G_{||}(\vec{R}_i,\vec{R}_j)=\langle\cos[2\pi(n_i-n_j)/p]\rangle$$
$$=\tfrac{1}{2}(\langle\sigma_i\sigma_j\rangle+\langle\tau_i\tau_j\rangle)\ \text{ for } p=4\,. \tag{3.8}$$

Because of the decoupling γ and ν take their usual Ising values, i.e., $\gamma_4=\gamma_2$ and $\nu_4=\nu_2$. Since, by scaling, we have $\gamma-\nu=(1-\eta)\nu$ where the exponent η for the critical-point decay satisfies $\eta<1$ for $d>1$, we see that the chiral field is *relevant* for all $d>1$ when $p=4$.

B. A domain-wall argument

It is instructive to rederive the $p=4$ result (3.7) by another route which illustrates the use of domain-wall concepts and serves as a basis for generalization to other values of p. To this end consider the interfacial tension and recall that it is defined as the excess free energy per unit area. More explicitly, for general p let $F^{n_-,n_+}(T,\Delta;L,A)$ denote the total free energy of a system of length L layers along the x axis, i.e., in the direction of the chiral field, and of $(d-1)$-dimensional cross-sectional area A, where the boundary condition $n_i=n_-$ is imposed on the Potts spins on layer $l=-\frac{1}{2}L$ while on the layer $l=+\frac{1}{2}L$ the condition $n_j=n_+$ is imposed. If a "twist" of one unit is imposed, so that $n_+-n_-=1$, then an interface of $A\,|\,B$ or $+1$ type and area A must be present in the system. Hence the interfacial tension can be defined by[51]

$$\Sigma_{+1}(T,\Delta)=[F^{0,1}(T,\Delta)-F^{0,0}(T,\Delta)]/A\,, \tag{3.9}$$

where it is understood that the thermodynamic limit, $L,A\to\infty$ is to be taken.

Since we are considering a phase with a discrete order parameter and, below T_c, finite correlation length we anticipate a more or less well-defined interface located centrally within the system. Nevertheless the interface, even if pinned at the transverse boundaries, is free to roughen and wander on a scale[42] which, for $d\leq 3$, diverges with A. However, provided we let L diverge sufficiently fast relative to A, the "collisions" of the interface with the ends of the system may be neglected.

Let us now utilize the scaling relation (3.5) for $(\partial\Sigma_{+1}/\partial\Delta)_0$. The total free energy $F^{0,0}(T,\Delta)$ describes a system with no interfaces and must be *even* in Δ; accordingly $(\partial F^{0,0}/\partial\Delta)_{\Delta=0}$ must vanish identically. (In the thermodynamic limit we should exclude $T=T_c^0$ but this has no effect on the argument.) From (3.9) and (3.5) we thus obtain

$$\frac{1}{A}\left[\frac{\partial F^{0,1}}{\partial\Delta}\right]_{\Delta=0}=\frac{1}{A}\left\langle\frac{\partial\mathscr{H}}{\partial\Delta}\right\rangle_{\Delta=0}^{0,1}\sim |t|^{\mu-\phi}\,, \tag{3.10}$$

where $\mathscr{H}$ denotes the chiral clock Hamiltonian (2.1) while the expectation value corresponds to the twisted boundary conditions with $n_+-n_-=1$. By invoking (asymptotic) translational invariance within the layers, the left-hand side reduces to a sum proportional to

$$Q=\sum_{l=-\frac{1}{2}L}^{\frac{1}{2}L-1}\langle\sin\{2\pi[n(l)-n(l+1)]/p\}\rangle_0\,, \tag{3.11}$$

where $n(l)$ denotes a typical Potts variable in layer l while $n(l+1)$ denotes its nearest neighbor in the next layer. The subscript 0 indicates the condition $\Delta=0$ and the superscript 0,1 has been dropped but must *not* be forgotten. Now, as explained, the interface, even if rough, will be confined to a region, say $-L' \leq l \leq L'$, where, asymptotically, $L' \ll L$. On the other hand, we may allow L' to become sufficiently large that we are assured that the layers around $l=\pm L'$ lie well within spatially uniform homogeneous phases within which the averages $\langle n(l)\rangle_0$, $\langle n^3(l)\rangle_0$, $\langle n^2(l)n(l+1)\rangle_0$, etc., are constant. Finally, the contributions from the end wall regions at $l \simeq \pm \frac{1}{2}L$ can be seen to cancel out by the $\sigma-\tau$ or end-to-end symmetries. It follows, therefore, that when $L \to \infty$ the limits of summation in (3.11) can be replaced by $-L'$ and $L'-1$, where the summand at these points effectively vanishes.

Now let us return to the case $p=4$ and notice that the boundary condition $n(-\frac{1}{2}L)=n_-=0$ translates via (3.6) into $\sigma(-\frac{1}{2}L)=\tau(-\frac{1}{2}L)=+1$, while the condition $n(\frac{1}{2}L)=n_+=1$ yields $\sigma(\frac{1}{2}L)=+1$ but $\tau(\frac{1}{2}L)=-1$. The sublattice of σ spins will, therefore, be *uniformally* magnetized (except near the ends) so that $\langle\sigma(l)\rangle_0$ is independent of l for $|l| \leq L'$ and equal to the Ising spontaneous magnetization $M_0(T)$, which vanishes as $|t|^\beta$. The sublattice of τ spins evidently contains an interface so that $\langle\tau(l)\rangle_0$ is nonuniform. However, by the arguments presented above, we have $\langle\tau(-L')\rangle_0=M_0(T)=-\langle\tau(L')\rangle_0$. Upon using (3.6) the sum in (3.11) becomes

$$\begin{aligned} Q &= \tfrac{1}{2}\sum_{l=-L'}^{L'-1}[\langle\sigma(l)\tau(l+1)\rangle_0-\langle\tau(l)\sigma(l+1)\rangle_0] \\ &= \tfrac{1}{2}\sum_{k=-K'}^{K'}\langle\sigma(2k)\rangle_0[\langle\tau(2k+1)\rangle_0-\langle\tau(2k-1)\rangle_0] \\ &\quad +\tfrac{1}{2}\sum_{k=-K'}^{K'}\langle\tau(2k)\rangle_0[\langle\sigma(2k-1)\rangle_0-\langle\sigma(2k+1)\rangle_0] , \end{aligned} \tag{3.12}$$

where we have factored the correlation functions of decoupled σ and τ spins, rearranged the first sum, and, for simplicity, assumed that $L'=2K'+1$ with K' integral. Since $\langle\sigma(l)\rangle_0$ is constant for $|l| \leq L'$ the last sum vanishes identically while the second sum simplifies to yield

$$\begin{aligned} Q &= \tfrac{1}{2}M_0(T)[\langle\tau(L')\rangle_0-\langle\tau(-L')\rangle_0] \\ &= [M_0(T)]^2 \sim |t|^{2\beta} . \end{aligned} \tag{3.13}$$

This unexpected reduction of $(\partial\Sigma_{+1}/\partial\Delta)_0$ for $p=4$ to the square of the spontaneous magnetization has been checked by explicit computation of the first few terms of the low-temperature expansion for $\Sigma_{+1}(T,\Delta)$ (using the techniques of Ref. 28).

Finally, by comparison with (3.5), we obtain the scaling relation

$$\phi=\mu-2\beta . \tag{3.14}$$

At first sight this seems quite different from (3.7). However, we may invoke Widom's general scaling argument[52] for the interfacial tension which yields

$$\mu=2\beta+\gamma_\Sigma-\nu_\Sigma . \tag{3.15}$$

The subscripts Σ have been introduced to emphasize that the compressibility and correlation length entailed are those directly involved in the free energy of formation of an interface.[52] For systems with Ising-like scalar order parameters these are just the normal, longitudinal susceptibility and correlation length and so $\gamma_\Sigma=\gamma$ and $\nu_\Sigma=\nu$; however, for systems like the clock models where the vectorlike order parameter can "twist" as it varies through an interface the *transverse* susceptibility and associated correlation length are the relevant ones as we will shortly demonstrate. Accepting $\gamma_\Sigma=\gamma_4$ and $\nu_\Sigma=\nu_4$ for $p=4$ one sees that (3.15) and (3.14) reproduce the original result, $\phi_4=\gamma_4-\nu_4$. It is worth emphasizing that Widom's relation (3.15) is *independent* of hyperscaling relations[50] such as $d\nu=2-\alpha$ or $\mu=(d-1)\nu$ which fail when $d>4$. Consequently, we expect (3.14) to be valid for all d as was (3.7).

C. Phenomenological theory: Large dimensionality

It should be possible to obtain correct results for large d, specifically for $d>4$, by invoking classical phenomenological or Landau theory. To this end we may introduce a discrete *complex* scalar order parameter,

$$\psi_j=\exp(2\pi i n_j/p) , \tag{3.16}$$

as an alternative representation of the clock models and then approximate this in the critical region by a continuously variable complex scalar field $\psi(\vec{r})$. An appropriate Landau-Ginzburg-Wilson Hamiltonian which should be in the same universality class as the p-state chiral clock model is then given by

$$\begin{aligned} \mathscr{H}[\psi(\vec{r})] = \int d^d r \Bigg[&\tfrac{1}{2}|\vec{\nabla}\psi(\vec{r})|^2+u_2|\psi(\vec{r})|^2+\Delta\left(\psi^*(\vec{r})\frac{\partial\psi(\vec{r})}{\partial x}-\psi(\vec{r})\frac{\partial\psi^*(\vec{r})}{\partial x}\right) \\ &-h_p[\psi^p(\vec{r})+\psi^{*p}(\vec{r})]+\sum_{k=2}^{\infty}u_{2k}|\psi(\vec{r})|^{2k}\Bigg] , \end{aligned} \tag{3.17}$$

where $\vec{\Delta}$ is parallel to the x axis, and $u_2 \sim (T-T_0)$ is to be regarded as the thermal field.

The classical phenomenological theory is generated, as usual, by approximating the free energy by the minimum of $\mathscr{H}$ over fields $\psi(\vec{r})$. When $\Delta=0$ this yields the standard classical, mean-field results for the usual exponents, namely, $\alpha=0$, $\beta=\frac{1}{2}$, $\gamma=1$, and $\nu=\frac{1}{2}$, the latter two exponents pertaining, as previously, to the longitudinal

correlations $\langle \psi^*(\vec{r})\psi(\vec{r}')\rangle$. The results are independent of p but it must be recalled that classical theory leads to a first-order transition, rather than a continuous Potts transition, when $p=3$.[56] For the moment, then, let us consider only $p \geq 4$ and examine the uniform *transverse* response below the critical point. Upon putting $\psi=\psi_0 e^{i\varphi}$ with real ψ_0 and φ, minimizing, and differentiating twice with respect to φ, one finds the transverse susceptibility is given by

$$\chi_\perp \propto 1/p^2 h_p \psi_0^{p-2} \sim |t|^{-(p-2)/2}, \tag{3.18}$$

so that $\gamma_\perp=\frac{1}{2}(p-2)$. Note that for $p=4$ we have $\gamma_\perp=\gamma=1$. The linear spatial dependent response follows in the usual way and yields $\nu_\perp=\frac{1}{2}\gamma_\perp=\frac{1}{4}(p-2)$ which, via the scaling relation $\gamma_\perp=(2-\eta_\perp)\nu_\perp$, reflects the standard classical result that $\eta_\perp=\eta=0$. It is clear for $p>4$ that the classical profile of an $A \mid B$ interface, in which the phase φ of the order parameter ψ changes from 0 to $2\pi/p$, becomes asymptotically just a simple arc, $|\psi|=\psi_0$, when $t\to 0$. In the Widom argument,[52] which is exact classically, we must thus take $\gamma_\Sigma=\gamma_\perp$ and $\nu_\Sigma=\nu_\perp$ in (3.15). This yields the surface-tension exponent

$$\mu_p=\tfrac{1}{4}(p+2), \quad p \geq 4 . \tag{3.19}$$

Of course, this may be checked by solving for the profile, say $\psi_\Sigma(\vec{r})$, in more detail. Likewise it is easily seen to hold also for $p=4$, as indicated, where it yields $\mu=1\frac{1}{2}$.

In order to determine the chiral crossover exponent ϕ it is clear that some property involving a spatially nonuniform order parameter must be examined [since, otherwise, this term in (3.17) vanishes identically]. Accordingly, let us ask for the effect of the chiral field on the interfacial tension Σ_{+1}. If the profile is decomposed into real and imaginary parts as

$$\psi(\vec{r})=\psi'(\vec{r})+i\psi''(\vec{r}), \tag{3.20}$$

we obtain from (3.10) and (3.17),

$$\frac{1}{A}\int d^d r \left\langle \psi'(\vec{r})\frac{\partial \psi''(\vec{r})}{\partial x}-\psi''(\vec{r})\frac{\partial \psi'(\vec{r})}{\partial x}\right\rangle_{\Delta=0}^{0,1} \sim t^{\mu-\phi}, \tag{3.21}$$

where the expectation value denotes, here, merely the minimization of the appropriate free energy subject to the unit twist boundary condition denoted, as before, by the superscript. Now for $p \geq 4$ and $t\to 0$, we can write the profile in the scaled form

$$\psi_\Sigma(\vec{r}) \equiv \langle \psi(\vec{r})\rangle_0^{0,1} \approx |t|^\beta P_p(x t^{\nu_\Sigma}), \tag{3.22}$$

where we leave open the identification of ν_Σ, while $P_p(w)$ is a universal scaling function. Upon substituting in (3.21) and noting that all fluctuations ($\langle AB\rangle-\langle A\rangle\langle B\rangle$) vanish classically we obtain

$$|t|^{2\beta}\int dw \left[P_p'(w)\frac{dP_p''(w)}{dw}-P_p''(w)\frac{dP_p'(w)}{dw}\right] \sim t^{\mu-\phi}. \tag{3.23}$$

The integral here is independent of t so that, *unless* it should happen to vanish, we recapture the result (3.14). Note also that the argument is actually independent of the value of ν_Σ (although it depends on the assumption, fully justified in the classical theory where we have seen that $\nu_\Sigma=\nu_\perp$, of a single relevant length scale). Substituting the classical values in (3.14) yields

$$\phi_p=\tfrac{1}{4}(p-2), \quad p \geq 4 . \tag{3.24}$$

Note that this result which should hold generally for $d \geq 4$ agrees, as it must, with the general result (3.7) for $p=4$ (where $\gamma_\perp=\gamma$ and $\nu_\perp=\nu$). It also coincides with the value that can be inferred from other approaches.[17,21,38]

D. General scaling argument

A perusal of the steps leading from the Hamiltonian (3.17) through (3.20)—(3.22) to the conclusion $\phi=\mu-2\beta$ reveals that the arguments may well transcend the classical phenomenological context, particularly for $p \geq 4$. The four crucial assumptions needed are the following: (i) that, following Widom,[52] some sort of "intrinsic" interfacial profile, $\psi_\Sigma(\vec{r})$, can be defined; (ii) that this profile scale with a single divergent correlation length; (iii) that one may neglect the correlations between the real and imaginary parts of $\psi(\vec{r})$ or, equivalently, between the longitudinal and transverse order parameter fluctuations; and (iv) that the integral over the scaling functions in (3.23) does not vanish identically.

Owing to roughening fluctuations (i) is open to question for $d \leq 3$ but does not invalidate the Widom argument for the exponent μ even when $d=2$. Assumption (ii) is very plausible for $p>4$, where the profile should still be characterized asymptotically by a constant amplitude $|\langle \psi(\vec{r})\rangle|$, but is open to more serious question for $p \leq 4$ (unless the model decomposes as discussed above) since the classical picture tends to suggest that the mean profile (if one can be defined) will probably entail a significant variation of amplitude and hence might possibly involve a second correlation length. It might be possible to address the issue of two distinct correlation lengths for $d=2$, $p=3$ by some analytic means but we have not attempted that. Regarding assumption (iii) all that is required is that the neglected fluctuation terms vanish faster than $|t|^{2\beta}$. Since coupling between the transverse and longitudinal fluctuations is primarily associated with the $h_p(\psi^p+\psi^{*p})$ term which, upon ϵ-expansion grounds seems likely to be irrelevant for $p>4$, this is also plausible. However, the conclusion is more dubious for $p \leq 4$ and might even fail for $p>4$ in low dimensions. Assumption (iv) is very plausible in the absence of some special reason of symmetry, etc., dictating a vanishing integral, and that should be equally reflected in (3.5).

A rather naive but direct scaling argument that capitalizes particularly on assumption (iii) above can be based directly on the form of the chiral term in (3.17) which, schematically,is $\Delta\int d^d r\, \psi'(\vec{r})\nabla\psi''(\vec{r})$. If we take the standard scaling postulates $\Delta\sim t^\phi$, $r\sim t^{-\nu}$, and $\nabla\sim t^\nu$ and, invoking (iii), *separately* set $\psi'\sim t^\beta$ and $\psi''\sim t^\beta$, we may invoke the overall scale-free character of the term to con-

clude that $\phi - d\nu + \nu + 2\beta = 0$ or

$$\phi = (d-1)\nu - 2\beta \,. \tag{3.25}$$

The Widom hyperscaling relation[52] $\mu = (d-1)\nu$ leads again directly to (3.14) while $d\nu = 2 - \alpha = 2\beta + \gamma$ yields the equivalent form $\phi = \gamma - \nu$ of (3.7). The danger of this approach is evident since one might likewise conclude that the energy $|\psi|^2$ scaled as $t^{2\beta}$ whereas in reality it scales as $t^{1-\alpha}$.

E. Low dimensions

The chiral field is relevant for all $p \geq 3$ at the symmetric critical point, $\Delta = T = 0$, of the one-dimensional p-state chiral clock model. This may be shown by an exact renormalization-group treatment of the model,[23] or by obtaining the multicritical scaling form (3.2) for the free energy. The latter calculation is presented in Appendix B. Because there is no low-temperature ordered phase, the chiral crossover-exponent relation $\phi = \mu - 2\beta$ cannot be checked explicitly for $d = 1$; however, it can be checked as $d \to 1+$, in which limit the Migdal-Kadanoff approximate renormalization group[53,54] is believed to be exact. In terms of the thermal and chiral renormalization-group eigenvalues, λ_T and λ_Δ (or y_T and y_Δ in Kadanoff's notation), at the appropriate fixed point, one has $\phi = \lambda_\Delta / \lambda_T$. To first order in $\epsilon = d - 1$, one finds (e.g., following Ref. 23) the eigenvalues $\lambda_T = \lambda_\Delta = \epsilon$, while for the uniform field one gets $\lambda_{h_1} = 1 + \epsilon$. These values lead to $\phi_p = 1$ for all $p > 2$, to $\beta = 0$, and via $\mu = 2\beta + \gamma - \nu$, to $\mu = 1$, thus confirming the general scaling argument for (3.14).

It is appropriate to sound a note of caution here, since for $p \geq 4$ and $2 < d < 4$, and for $p > 4$ and $d \geq 4$ the field h_p in (3.17) is *irrelevant* so that the symmetric clock transition is governed by the XY-like fixed point[38,55] (which is *not* the case for $d \leq 2$). In these cases the surface-tension exponent and the effective chiral crossover exponent are determined not only by the renormalization-group eigenvalues λ_T and λ_Δ (which has the value unity in these cases) but *also* by the irrelevant or correction-to-scaling eigenvalue λ_{h_p} associated with h_p, as seen from the analysis of Aharony and Bak.[38]

F. Series analysis

The chiral exponent ϕ for the two-dimensional three-state clock model has been estimated numerically[28] using low-temperature series expansions for $(\partial \Sigma_+ / \partial \Delta)_{\Delta=0}$ and *also* high-temperature expansions for the cross derivative $(\partial^2 \chi / \partial q \, \partial \Delta)_{q=\Delta=0}$ where $\chi(T, \Delta; q)$ is the usual momentum-dependent susceptibility which is expected to scale as

$$\chi(T, \Delta; q) \approx t^{-\gamma} X\left[\frac{\Delta}{t^{\phi}}, \frac{q}{t^{\nu}}\right] . \tag{3.26}$$

The resulting estimate[28] $\phi = 0.19 \pm 0.06$ $(d = 2)$, describes well *both* high- and low-temperature series. However, it is significantly smaller than would be concluded if the relation $\phi = \mu - 2\beta$ were accepted since, on the basis of the proposed exact Potts exponents,[35,36] and Widom's hyperscaling relation[52] $\mu = (d-1)\nu$, it yields $\phi = \frac{11}{18} \simeq 0.61$. (The Migdal-Kadanoff renormalization group on a Berker or fractal lattice with $d_{\text{eff}} = 2$ yields $\phi_3 = \frac{1}{2}$.[23]) It may be significant that a similar difference of about 0.4 was found between the low-temperature series estimates[56] for γ and $\gamma_\perp$, the longitudinal and transverse susceptibility exponents of the three-state Potts model.

The disagreement between the series estimate $\phi_3 \simeq 0.2$ and the scaling-relation prediction $\phi_3 \simeq 0.6$ leads us, for $p = 3$ and $d = 2$, to doubt some of the assumptions needed in the scaling argument. We believe those most suspect are, first, the neglect of correlation between longitudinal and transverse fluctuations and, second, the assertion that the integral over the profile scaling function in (3.23) does not vanish identically. However, we have no suggestions for going beyond these assumptions in general. For the special case $p = 4$, $d = 2$, which reduces to the relatively well-understood Ashkin-Teller model in the absence of chiral symmetry breaking, Schultz[16] has recently calculated the chiral crossover exponent ϕ_4 along the entire critical line. His result,

$$\phi_4 = \frac{3\nu}{2} + \frac{1}{4} - \frac{\nu^2}{2\nu - 1} \,,$$

as parametrized by the correlation length exponent ν, agrees, of course, with the above analysis at the decoupling point, $\nu = 1$.[39] However, our simple scaling relation (3.14) does not work anywhere else along the critical line of the two-dimensional Ashkin-Teller model. Thus the general scaling argument leading to (3.14), which is certainly valid for $d \geq 4$ and probably remains valid for $d = 3$, has a very restricted applicability for $d = 2$. It is worth noting that for the *four*-state Potts model, where $\nu = \frac{2}{3}$, Schulz[16] finds that chiral-symmetry breaking is actually *irrelevant*, with $\phi_4 = -\frac{1}{12}$.

G. Hexagonal phases

A Landau-Ginzburg-Wilson Hamiltonian with symmetry appropriate for modeling the melting of a commensurate $\sqrt{3} \times \sqrt{3} R 30°$ phase of a general triangular lattice gas is

$$\mathcal{H}[\psi(\vec{r})] = \int d^2\vec{r} \{ \tfrac{1}{2} |\vec{\nabla}\psi|^2 + u_2 |\psi(\vec{r})|^2 + \Delta[\psi^*(\vec{r}) \nabla_1 \nabla_2 \nabla_3 \psi(\vec{r}) - \psi(\vec{r}) \nabla_1 \nabla_2 \nabla_3 \psi^*(\vec{r})] + h_3[\psi^3(\vec{r}) + \psi^{*3}(\vec{r})] + u_4 |\psi(\vec{r})|^4 + \cdots \} \,, \tag{3.27}$$

where Δ now represents a *triaxially chiral* symmetry breaking field. The spatial gradient operators ∇_1, ∇_2, and ∇_3 act at mutual angles of $2\pi/3$ parallel to the nearest-neighbor directions specifying the triangular lattice. The form of the lowest-order chiral symmetry breaking operator here makes it evident why we have dubbed it "triaxial". (Note that operators of the schematic form $\nabla_1 \psi \nabla_2 \psi \nabla_3 \psi$, etc., may arise in higher order; see also

Hornreich *et al.*[57]) If the previous scaling arguments are applied, most readily in the naive form leading to (3.25), the *triaxial* chiral crossover exponent is found to be

$$\phi = -\nu - 2\beta = \mu - 2\nu - 2\beta \,, \tag{3.28}$$

for which the accepted Potts values[35,36] yield $\phi = -\frac{19}{18}$. This is strongly negative, suggesting that triaxially chiral symmetry breaking is irrelevant at the three-state Potts-model critical point. This conclusion is consistent with Baxter's exact calculations[29,40,41] for a gas of hard hexagons on a triangular lattice where such terms should appear in the Landau-Ginzburg-Wilson Hamiltonian but pure Potts exponents are found. (See further in Sec. IV below.)

IV. SCALING AT CHIRAL PHASE TRANSITIONS

In the preceding section we have demonstrated that uniaxially chiral symmetry breaking is a relevant perturbation at the p-state clock-model critical point. This means that for any nonzero chiral field the melting of the commensurate phase must, in a renormalization-group picture, be governed by a different fixed point than that which controls the pure, symmetric clock-model critical point. The symmetric critical point is therefore *multi*critical and the chiral field induces crossover to a melting transition which is expected to belong to a different universality class. As is discussed in detail in the following section, the crossover should be to a commensurate-incommensurate transition for most values of p and d. However, for one case of physical interest, namely the three-state chiral clock model in two dimensions, there is some numerical evidence based on Monte Carlo simulations[25] and series expansions[27] that the commensurate phase melts directly into the disordered phase for sufficiently small, but nonzero chiral fields. Since the chiral field, Δ, is relevant, melting in the presence of a nonzero chiral field should be in a different universality class than that of the pure, $\Delta = 0$, three-state model. (Although it should be recalled that examples of multicritical crossover are known where the "new" transition is actually in the same universality class as the original transition, for example, in Ising models of two coupled layers.[39])

Indeed we have proposed[37] and argue in more explicit detail in Sec. VI below that such melting of a $p = 3$ commensurate phase directly into a disordered, fluid phase in the presence of uniaxially chiral symmetry breaking should be in a new chiral universality class. In this section we discuss scaling at such chiral phase transitions in order to emphasize how they should differ from phase transitions in the usual, nonchiral universality classes and how they might thus be detected experimentally.

Since we are interested in continuous transitions let us consider the behavior of the structure factor $S(\vec{q};T,\zeta)$ in the disordered phase, where ζ might again stand for the chemical potential of adsorbate particles or represent changes in the uniaxial chiral field $\vec{\Delta}$ in clock models or the triaxially chiral field in models appropriate for hexagonal phases (see Sec. II). In the vicinity of the critical line $T_c(\zeta)$, the structure factor will exhibit peaks which reflect the incipient commensurate ordering which is established below the transition. Let us focus on one of these peaks located in momentum space in the neighborhood of the location, $\vec{G}$, of a Bragg peak of the commensurate-phase superlattice and write

$$\vec{q} = \vec{G} + \hat{x}\,\Delta q \,, \tag{4.1}$$

where the unit vector $\hat{x}$ in reciprocal space is chosen so that the peak appears sharpest in scans taken in directions parallel to $\hat{x}$. The width, $\kappa_x(T,\zeta)$, of the peak observed, say at "half-height," represents a measure of the corresponding correlation length. Thus as

$$\dot{t} = [T - T_c(\zeta)]/T_c(\zeta) \tag{4.2}$$

becomes small, we expect the behavior

$$\kappa_x(T,\zeta) \approx |\dot{t}|^{\nu}/a \sim 1/\xi \,, \tag{4.3}$$

where ν is the appropriate (in the case of interest, say, *chiral)* critical exponent, while the amplitude a is, generally, a length of order of the underlying lattice spacing.

For many systems, including most of the simple lattice models (e.g., Ising, Potts, n vector, etc.) the structure factor is symmetric about $\vec{G}$ and one finds the maximum occurs at $\vec{q} = \vec{q}_{\max} = \vec{G}$. In the chiral systems in which we are interested, however, we must expect this symmetry to be broken so that $\vec{q}_{\max}(T,\zeta)$ may be significantly incommensurate with the underlying reciprocal lattice. It is then appropriate to measure the *incommensurability* by

$$\bar{q}(T,\zeta) = |\vec{q}_{\max}(T,\zeta) - \vec{G}| \,, \tag{4.4}$$

which, as the transition is approached, should vanish so that we may write

$$\bar{q}(T,\zeta) \sim |\dot{t}|^{\bar{\beta}} \tag{4.5}$$

(compare with Ref. 42 and references cited therein.)

More generally, as $\dot{t} \to 0$, we expect the structure factor to scale asymptotically[50] as

$$S(\vec{q};T,\zeta) \approx |\dot{t}|^{-\gamma} D(\Delta q\, a/|\dot{t}|^{\nu}) \,, \tag{4.6}$$

where γ is the appropriate susceptibility exponent, while the scaling function $D(w)$ should be universal. Now for all the normal universality classes, namely Ising, Potts, clock, etc., the scaling function will be symmetric about $w = 0$ with a maximum *at* $w = 0$. Thus any asymmetry about $\vec{q} = \vec{G}$ observed in $S(\vec{q};T,\zeta)$ near a transition in these universality classes can be due *only* to *corrections* to the leading asymptotic scaling behavior. For such transitions, therefore, one must observe that $\bar{q}$ vanishes more rapidly than naive scaling might suggest. In other words the inequality $\bar{\beta} > \nu$ should be satisfied and the ratio $\bar{q}(T,\zeta)/\kappa_x(T,\zeta)$ of incommensurability and width should vanish asymptotically as $\dot{t} \to 0$.

An exact theoretical calculation which bears out this conclusion has been presented by Baxter and Pearce,[41] who studied the correlation functions near the melting transition of hard hexagons on a triangular lattice. The original arguments[33,34] which overlook the coupling of spin and lattice symmetries, suggest the transition should be of three-state Potts character. This is supported by our

analysis in Sec. III G, which indicates that the asymptotic triaxially chiral symmetry breaking operator should be *irrelevant* at the pure ($p=3$) Potts point so that, at least for *sufficiently small* triaxial chirality, the universality class should not change. Baxter and Pearce[41] found, in the first place, $\nu=\frac{5}{6}$, which agrees with the anticipated Potts exponent[35,36] (the calculated thermodynamic exponents[29,40] also agree). In the second place, they obtain an incommensurability exponent $\bar{\beta}=\frac{5}{3}$; this evidently exceeds ν in accordance with our conclusions.

On the other hand, for a transition in a *chiral* universality class we must expect that the critical fluctuations giving rise to the near-commensurate peak in $S(\vec{q})$ should reflect the chirality in an *intrinsic* scaling manner. Thus in a renormalization-group picture, chiral behavior will be characterized by a nonvanishing value of the chiral symmetry breaking field present at the fixed point itself. In more physical terms, the preference for, say, "heavy" domain walls in the chiral commensurate phase (as discussed in Sec. II but see also Sec. VI below), should be mirrored in the disordered phase. Heavy walls resemble discommensurations as observed in incommensurate, floating phases,[5,14–16,42] and hence naturally impose a nonzero incommensurability $\bar{q}(T,\zeta)$. We conclude that the scaling function, $D(w)$, should, for a chiral transition, be asymmetric with, furthermore, a maximum at a nonzero value of its argument, say, $w=w_0$.

It follows from these arguments that a chiral transition should be signaled rather unambiguously by the *nonvanishing* of the scaled incommensurability $\bar{q}/\kappa_x$ as $t\to 0$, rather we expect

$$\bar{q}(T,\zeta)/\kappa_x(T,\zeta)\to w_0\neq 0\ , \tag{4.7}$$

as $t\to 0$, where, for a given chiral class, w_0 should be a *universal* number. As a consequence of this the incommensurability exponent should satisfy

$$\bar{\beta}=\nu\ . \tag{4.8}$$

Such scaling behavior is, indeed, found in the chiral clock models and appears to be at least consistent with the data in one experimental study.

To be specific, near the $T=0$ ordering of the one-dimensional p-state chiral clock model in the presence of a chiral field ($\Delta\neq 0$) the structure factor does indeed scale as in (4.6), as shown in Appendix B. When $T\to 0$ the scaled incommensurability, $\bar{q}/\kappa_x$, is found to approach the universal limiting value

$$w_0(p)=\mathrm{sgn}(\Delta)\cot(\pi/p)\ , \tag{4.9}$$

for $0<|\Delta|<\frac{1}{2}$. This yields $w_0(2)=0$, as it should, and $w_0(3)=1/\sqrt{3}\approx 0.577$, $w_0(4)=1$, etc. In addition to this exact result for $d=1$, a Migdal-Kadanoff approximate renormalization-group[53,54] treatment of the three-state chiral clock model for $d>1$ showed explicitly that for $d_{\mathrm{eff}}\leq 2$ the chiral ($\Delta\neq 0$) portion of the continuous commensurate-to-fluid melting transition was governed by a simple fixed point with only one relevant eigenvalue.[23] This eigenvalue served in the standard way (entailing hyperscaling[50]) to determine both the correlation length and incommensurability exponents so confirming the relation $\bar{\beta}=\nu$. (The analysis again yields a positive value for w_0 of order unity.)

On the experimental side, Moncton and co-workers,[4] using high-resolution synchrotron x-ray techniques, have studied the behavior of Kr on graphite near the apparent commensurate-to-incommensurate transition. The commensurate $\sqrt{3}\times\sqrt{3}R30°$ phase extends[3] up to temperatures of about 130 K. In constant-filling scans, in which T and ζ change together, they found, on crossing the commensurate phase boundary near 95 K, a narrow interval in which a highly correlated fluid phase (with $\xi\gtrsim 100$ Å) exists between the commensurate and incommensurate phases as indicated schematically in Fig. 4. (The existence of such an intervening fluid phase has been explained theoretically on the basis of domain-wall arguments.[5]) In the corresponding profiles of the diffraction peak the incommensurability, $\bar{q}$, is clearly observable, as is the width κ_x. The results of Moncton *et al.*[4] suggest that the ratio $\bar{q}/\kappa_x$ approaches a nonzero limiting value of, say, $w_0\simeq 1.0\pm 0.5$ at the fluid-commensurate phase boundary.

The nonzero value of the limit w_0 seen in these experiments is, as explained, indicative of the intrinsically chiral nature of the transition. At first sight this is paradoxical theoretically because we have argued that the triaxial chirality appropriate for the corresponding hexagonal $\sqrt{3}\times\sqrt{3}$ phases should be *irrelevant* at the pure Potts point. However, as stressed, the conclusion that the melting transition should remain in the pure Potts universality class is valid only if the triaxially chiral field is not too

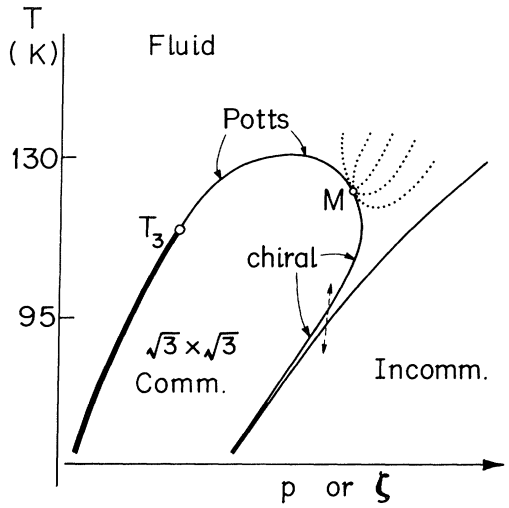

FIG. 4. A somewhat schematic phase diagram of Kr on graphite showing fluid, $\sqrt{3}\times\sqrt{3}R30°$ commensurate, and incommensurate phases. The bold line indicates a first-order melting transition, while the remaining phase boundaries represent continuous melting. The tricritical point T_3 separates the first-order and continuous portions of the commensurate melting boundary, while the proposed new multicritical point, M, separates the continuous portion into segments in Potts and chiral universality classes, as indicated. The dashed line indicates (*schematically*) the path taken in the Moncton *et al.* experiment, which we interpret as indicating chiral melting in that region. The dotted curves emerging from M represent (again schematically) expected loci of constant $\bar{q}/\kappa_x$ for $0<\bar{q}/\kappa_x<w_0$ (see Secs. IV and V).

large. The experimental data, if accepted at face value, indicate a chiral region on the melting curve as shown in Fig. 4. One must thus conclude[37] that the triaxial symmetry breaking exceeds a threshold corresponding to a multicritical value, represented by the point M in Fig. 4. For symmetry breaking below this threshold the melting transition *is* governed by the pure Potts fixed point. This question is taken up again in the next section.

Moncton and co-workers[4] also report an estimate of the incommensurability exponent, namely, $\bar{\beta}\simeq\frac{1}{3}$. However, much of the data used to obtain this estimate lies as far as 5 K away from the transition, and therefore well outside of the asymptotic scaling regime, which must be very small because of the close proximity of the fluid-to-incommensurate phase transition. The width of the scaling regime, in which the asymptotic power laws provide a reasonably accurate representation, may be estimated by observing where the scaling law $\bar{q}\sim\kappa_x$ is approximately obeyed. This range appears to be less than 0.5 K in the available data.[4] Thus the fitted exponent $\beta\simeq\frac{1}{3}$ must be regarded as an *effective* exponent, presumably determined to some extent by properties of the incommensurate phase. In general, the true asymptotic incommensurability exponent at the fluid-to-commensurate transition should, if one accepts the scaling arguments, satisfy the inequality $\bar{\beta}\geq\frac{1}{2}$. This follows from the conclusion $\beta\geq\nu$ and the fact that on rather general grounds one expects $\nu\geq\frac{1}{2}$ for $d=2$. This bound on ν arises from hyperscaling, $\nu=(2-\alpha)/d$, and the requirement that $\alpha\leq 1$ because the energy density, which varies as $t^{1-\alpha}$, cannot diverge.

We turn next to a more extensive discussion of the anticipated chiral phase diagrams.

V. PHASE DIAGRAMS

A plausible phase diagram for Kr on graphite, based on the present experimental evidence[1,3,4] and the preceding analysis, is shown in Fig. 4. The $\sqrt{3}\times\sqrt{3}R30°$ commensurate phase exists only for temperatures below about 130 K and then only for an intermediate range of vapor pressure (or chemical potential or coverage).[3] The commensurate-phase boundary on the low-vapor-pressure side of this phase represents a melting transition into a fluid; this transition is of first order for temperatures below the tricritical point, marked T_3, but continuous for higher temperatures.[1,2] On the high-vapor-pressure side the commensurate phase still melts continuously into a fluid at sufficiently high temperatures;[4] for lower temperatures there may well be a direct commensurate-to-incommensurate transition and corresponding multicritical point (not shown).[5,58] The intrusion of the fluid phase between the commensurate and incommensurate phases was observed by Moncton *et al.*[4] and explained by Coppersmith, Fisher, Halperin, Lee, and Brinkman[5] on the basis of an instability of the weakly incommensurate phase to dislocation-mediated melting (see also Ref. 19). Recent molecular-dynamics simulations by Abraham *et al.*[47] also indicated the presence of such an interval of fluid phase at approximately 100 K.

It was argued in Sec. III that the triaxially chiral symmetry breaking present in a $\sqrt{3}\times\sqrt{3}$ phase such as Kr on graphite is irrevelant at the pure Potts critical point. Thus the commensurate melting transition should remain in the universality class of the three-state Potts model for sufficiently weak symmetry breaking. As explained in Sec. II, the pressure or chemical potential must couple directly to the chiral symmetry breaking terms so that weak symmetry breaking should correspond to low or intermediate pressures, on some appropriate scale. Thus we expect the continuous melting transition of the $\sqrt{3}\times\sqrt{3}$ commensurate phase to be in the Potts universality class near the tricritical point T_3 and over some segment of the high-temperature portion of the phase boundary, where the melting is clearly not pressure-driven. On the other hand, our scaling arguments lead us to interpret the data of Moncton *et al.*[4] as indicating that commensurate melting on the high-pressure portion of the phase boundary near 95 K is in a chiral universality class. The simplest phase diagram consistent with these expectations must contain a new multicritical point, labeled M in Fig. 4, where crossover from Potts to chiral melting occurs.

This postulated multcritical point might be detected in an experiment or simulation by observing the behavior of the ratio $\bar{q}/\kappa_x$ in the fluid phase as discussed in the preceding section. This ratio should vanish on the Potts portion of the commensurate-phase boundary but attain a nonzero limit w_0 at the chiral portion of the phase boundary. Thus in the vicinity of the multicritical point the ratio must vary rapidly. Furthermore, loci of constant $\bar{q}/\kappa_x$, for all values of the ratio satisfying $0<\bar{q}/\kappa_x<w_0$, must emerge from the multicritical point, as illustrated by the dotted curves in Fig. 4. Such behavior might be observable in either Kr on graphite or, possibly, in the triaxially chiral Potts model embodied in the Hamiltonian (2.3).

Let us now discuss the phase diagrams of the *uniaxially* chiral clock models defined by (2.1). As the dimensionality, d, and the state number, p, are varied, the phase diagram of the p-state chiral clock model or any other system exhibiting a $p\times 1$ commensurate phase, may take on various forms as is discussed by Ostlund[22] and by Aharony and Bak.[38] Some of the possibilities are illustrated in Fig. 5. As above, we assume that no first-order transitions occur. (In experimental realizations this assumption may well fail in various regions of the phase diagram.) In all cases with $p\geq 3$ the symmetric ($\Delta=0$) melting point of the commensurate phase is multicritical, as is demonstrated in Sec. III. Commensurate melting for $\Delta\neq 0$ is therefore in a different universality class. Near the multicritical point the melting line, $T_M(\Delta)$, should, by (3.2) or (3.3), have a contribution varying as $|\Delta|^{1/\phi_p}$. Thus for $\phi_p<1$ we expect the commensurate-phase boundary to be smooth at the symmetric multicritical point, while for $\phi_p>1$ it should have a cusp as shown in Figs. 5(a) and (b), respectively.

In mean-field theory, which should apply for $d\geq 4$, the commensurate phase melts directly into the fluid only when $\Delta=0$. The relevant chiral field causes crossover from this simple direct transition to a *double transition*, consisting of a lower commensurate-incommensurate transition and followed, at a higher temperature, by an incommensurate-fluid transition.[17,21,38] The chiral crossover exponent is $\phi_p=(p-2)/4$, so Fig. 5(a) should apply

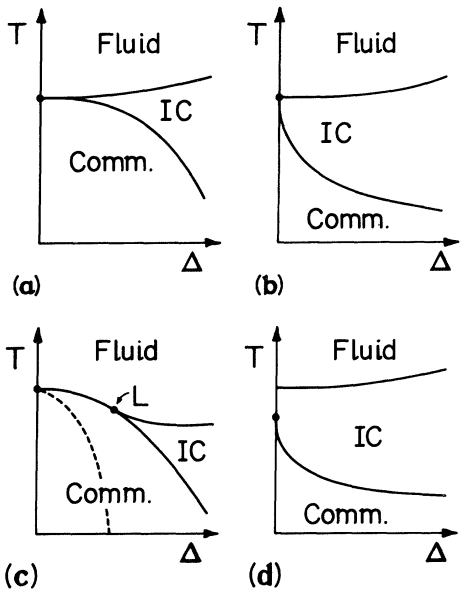

FIG. 5. Schematic phase diagrams for the p-state chiral clock model with Hamiltonian (2.1) for various dimensionalities, d, and values of p: (a) $d \geq 4$, $p=4$ or 5 and, possibly, $p=4$, $d=2$ or 3; (b) $d \geq 3$, $p > 6$ and $d=3$, $p=6$; (c) Probable phase diagram for $d=2$, $p=3$ with a wetting line (dashed); (d) $d=2$, $p \geq 5$. Each phase diagram is invariant under $\Delta \Longrightarrow -\Delta$ and contains fluid, commensurate, and incommensurate (*IC*) phases as well as a multicritical point at $\Delta=0$. A Lifshitz multicritical point, L, occurs in (c).

for $p=4$ and 5. (Recall that $p=3$ yields a first-order transition in mean-field theory.) Likewise, Fig. 5(b) should describe the behavior for $p>6$. A renormalization-group $\epsilon=4-d$ calculation by Aharony and Bak[38] indicates that ϕ_p increases for all p as the dimensionality is reduced below $d=4$. Thus in three dimensions we expect Fig. 5(b) to apply for $p \geq 6$. For $p=5$ it is unclear from the ϵ expansion[38] whether or not ϕ_5 exceeds unity at $d=3$; thus either Fig. 5(a) of Fig. 5(b) might apply. For $p=4$, $d=3$ it is known[39] that $\phi_4 \simeq 0.6$, so Fig. 5(a) is appropriate; however, for this case we know of no argument that rules out the possibility of a Lifshitz multicritical point occurring and thereby leaving a direct commensurate-fluid transition for small, nonzero Δ, as in Fig. 5(c).

For two dimensions the chiral clock-model phase diagrams have already been discussed by Ostlund.[22] He points out that for $p \geq 5$ the symmetric ($\Delta=0$) clock model should no longer have a direct commensurate-to-fluid transition.[49] The incommensurate phase, which is "accidentally commensurate" for $\Delta=0$ (see José *et al.*[49]), separates the commensurate and fluid phases for all Δ as illustrated in Fig. 5(d). The commensurate melting transition at $\Delta=0$ should be of the Kosterlitz-Thouless type[49] and the relevant chiral field causes crossover to a commensurate-incommensurate transition of the type discussed by Pokrovsky and Talopov.[14–16]

Finally, for $p=3$ and 4 in two dimensions the commensurate phase does melt directly into a fluid for $\Delta=0$ and we have $\phi_p < 1$, as demonstrated in Sec. III, hence either Fig. 5(a) or Fig. 5(c) should apply. For $p=3$ the numerical evidence[25,27] suggests that a Lifshitz point, at which commensurate, incommensurate, and fluid phases meet, occurs at nonzero Δ, as in Fig. 5(c). For the ANNNI model, which has $p=4$ near its decoupling point,[39] phase diagrams with (see Ref. 20) and without[59] Lifshitz points have been proposed on the basis of numerical studies. If the Lifshitz point does actually occur, as certainly seems likely for $p=3$, then the commensurate melting transition boundary between the symmetric multicritical point and the Lifshitz point should be in a new chiral universality class as discussed in the preceding section.

How might a chiral melting transition, in which the commensurate phase melts directly into a fluid, be differentiated from a double transition with a narrow interval of weakly incommensurate phase? The analysis of the preceding section suggests that the most obvious difference is in the behavior of the ratio $\bar{q}/\kappa_x$ in the near-critical fluid phase. If the fluid orders first into an incommensurate phase, then κ_x will vanish *before* $\bar{q}$ does and the ratio will diverge. This should be contrasted with a chiral transition, at which the ratio $\bar{q}/\kappa_x$ should go to a constant. Such studies of both model and experimental systems might help answer the question of the existence of a Lifshitz point for $p=3$ and 4.

VI. DOMAIN-WALL WETTING TRANSITIONS AND CROSSOVER

In a system with p distinct commensurately ordered domains equivalent under cyclic permutation, such as the chiral clock models with Hamiltonian (2.1), there will, as discussed in Sec. II, be $p-1$ inequivalent types of domain wall with tensions $\Sigma_q(T,\vec{\Delta};\theta)$. Here $\Delta=|\vec{\Delta}|$ represents the magnitude of the chiral field which we may associate, as in (2.2), with the deviation, $\zeta-\zeta_0(T)$, of the chemical potential, etc., from the ideal, effectively zero-chirality locus $\zeta_0(T)$, while θ represents the orientation of the wall as specified, say, by the angle (or angles for $d>2$) determining the mean normal to the wall. As before, the subscript $q=1,2,\ldots,p-1$ is defined by

$$q = n_+ - n_- \pmod{p}\,, \tag{6.1}$$

where n_+ and n_- represent the predominant Potts-clock spin states in the domains on the "right" or positive side of the wall and on the "left" or negative side, respectively. We will discuss the variation of the tensions $\Sigma_q(T;\vec{\Delta};\theta)$ in the (T,Δ) plane demonstrating that *wetting transitions* of the domain walls may occur and, indeed, should occur if the commensurate phase undergoes continuous chiral melting. Thereby we will also see microscopically why chiral melting represents a new universality class.

A. Stability considerations

Let us observe first that to ensure the thermodynamic stability of a q wall its tension must satisfy the inequality

$$\Sigma_q(T,\vec{\Delta};\theta) \le \Sigma_{r_1}(T,\vec{\Delta};\theta)+\Sigma_{r_2}(T,\vec{\Delta};\theta) + \cdots +\Sigma_{r_s}(T,\vec{\Delta};\theta)$$

$$\text{with } r_1+r_2+\cdots+r_s=q \pmod p , \quad (6.2)$$

for all q and all possible decompositions $\{r_j\}$. This fact, which simply generalizes the analogous inequality for the interfacial tensions in three-phase fluid systems,[48] may be illustrated most readily by considering the simplest case $q=2$ which corresponds to a wall separating, say, an $n_-=0$ domain from an $n_+=2$ domain. The system with just these two domains and the orientation of their boundary asymptotically specified must certainly assume the configuration of overall lowest free energy. One candidate for such a configuration is that in which a *layer* of $n_0=1$ domain exists *between* the $n_-=0$ and $n_+=2$ domains as in Fig. 6(b). Clearly, this would entail two $q=1$ walls with a total excess free energy per unit wall area of $2\Sigma_1$. Thus a $q=2$ wall might, in its actual structure, *consist* of *two* $q=1$ walls separated by an intruding layer and, in fact, it *will* do so if that state yields the lowest total free energy. This immediately yields the inequality $\Sigma_2 \le 2\Sigma_1$; the obvious generalization of the argument leads to (6.2).

B. Wetting transitions

When, for some decomposition $\{r_j\}$; the *equality* holds in (6.2) over some range of T and $\vec{\Delta}$, we must conclude that the putative q wall has in fact decomposed into two, or possibly more, walls of greater stability separated by one or more (as the case may be) intruding layers: In such a case the q wall is said to be "wet" (by the intruding layers). A locus in the (T,Δ) plane on which equality in (6.2) may be changed to *in*equality by infinitesimal changes of T and Δ, clearly represents a line of *wetting transitions.*[60,61]

For simplicity let us examine further the simplest case $p=3$ for which there are just the two independent tensions $\Sigma_1 \equiv \Sigma_+$ and $\Sigma_2 \equiv \Sigma_-$. In the absence of a chiral field ($\Delta=0$) the full Potts symmetry dictates $\Sigma_+(T,0;\theta)\equiv\Sigma_-(T,0;\theta)$. Now we introduce a chiral field $\vec{\Delta}$ parallel to the x axis. If the walls are oriented so that they are *transverse* to the chiral field (i.e., so that the x direction does not lie *in* the "plane" of the walls), the tension Σ_- will increase as Δ rises from zero while Σ_+ decreases. The difference $(2\Sigma_+-\Sigma_-)$ therefore falls quite sharply from its $\Delta=0$ value, $\Sigma_+=\Sigma_-$. This in turn lowers the cost in free energy of a *fluctuation* in the structure of the $[-]$ or $q=2$ wall in which it splits *locally* into two $[+]$ or $q=1$ walls. Some such fluctuations are illustrated schematically in Fig. 6(a).[28] As Δ is further increased such fluctuations become more frequent still and may well eventually diverge as the $[-]$ wall becomes unstable against splitting over its entire length (or area) into two $[+]$ walls with the intrusion of a layer of new, intermediate, $n_0=1$, domain [see Fig. 6(b)]. This phenomenon

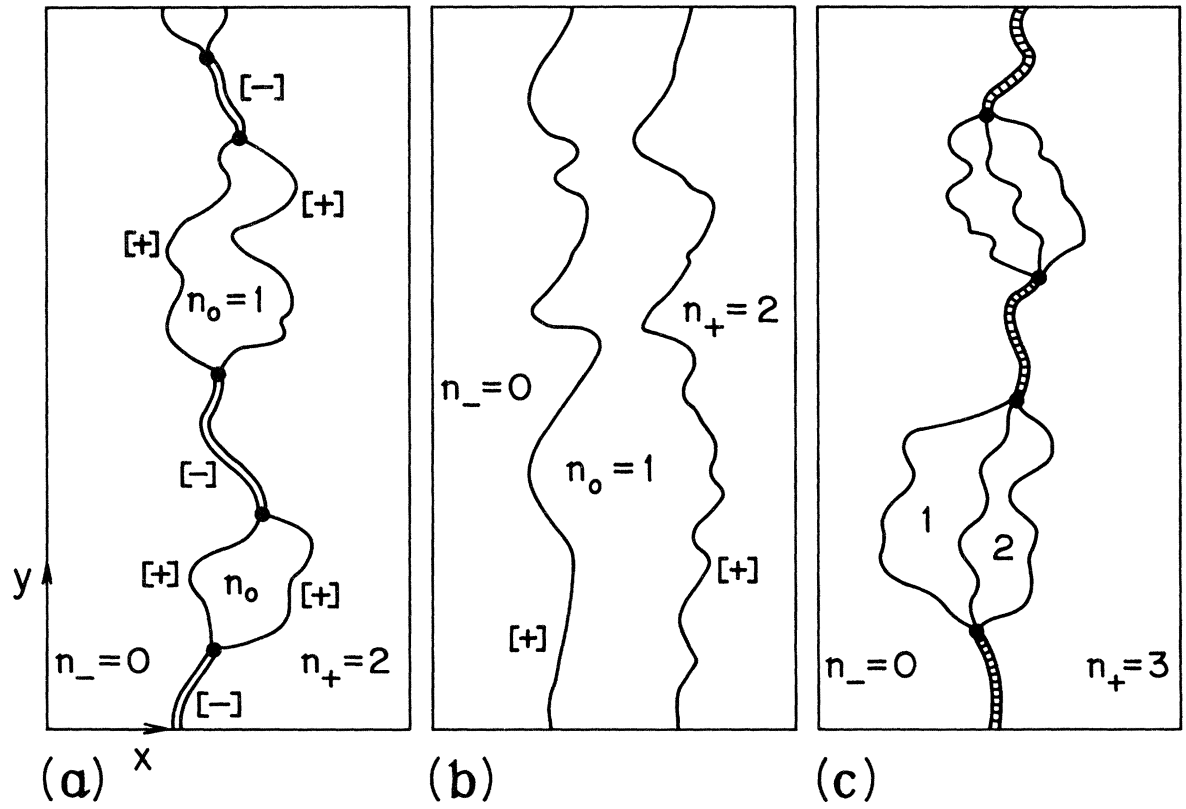

FIG. 6. Portrayals of dominant fluctuations in domain walls. (a) A $[q=2]\equiv[-]$ wall in a uniaxial $p=3$ system undergoing fluctuations into double-stranded bubbles of $[+]\equiv[1]$ wall leading, ultimately, to a wetting transition with, (b), complete intrusion of the intermediate phase characterized by the predominant occupation of the microstate $n_0=1$. (c) Fluctuations in a $[q=3]$ wall in, say, a $p=4$ system in the form of q-stranded "bananas."

then represents a *continuous,* or *critical wetting transition.* A detailed analysis of the $(p=3)$-state chiral clock model at low temperatures on a $(d=2)$-dimensional lattice shows that such a continuous domain-wall wetting transition does, indeed, occur[28] Furthermore, one finds that the wall wetting transition occurs *inside* the commensurate region of the (T,Δ) plane, well *away* from the bulk melting line as illustrated in Fig. 5(c) (dashed locus). This is analogous to critical wetting transitions predicted on the basis of mean-field and classical phenomenological arguments for bulk fluid mixtures which should, likewise, occur independently of bulk criticality.[62–65] The explicit calculations of Ref. 28 reveal the critical exponents describing the wetting transition for the case $p=3, d=2$. We will shortly present more general phenomenological arguments that yield the same values for this case but show that, in certain other circumstances, two-dimensional domain-wall wetting transitions may be of first order (as also anticipated[60,63–65] for fluids with $d \geq 3$). Before that, however, let us return to the case of general $p \geq 3$.

Consider, for example, a $[q=3]$ wall in a $p=4$ system. At a wetting transition such a wall might decompose into a $[q=2]$ wall and a $[q=1]\equiv[+]$ wall (in two possible ways) so that the equality $\Sigma_3=\Sigma_1+\Sigma_2$ will hold at and beyond the transition. Alternatively, the predominant fluctuations, as illustrated in Fig. 6(c), might lead it to decompose into *three* $[q=1]$ walls, the equality $\Sigma_3=3\Sigma_1$ applying thereafter. The former, twofold decomposition can, clearly, occur only if the Σ_2 wall is not already wet or *at* its wetting transition. Similar considerations for a $p=5$ system reveal just three possibilities for a $q=4$ wall which might decompose (i) into two $q=2$ walls, (ii) into a $q=3$ and a $q=1$ wall (in two ways), or (iii) into four $q=1$ walls, or symbolically,

$$\text{(i) } [4]\rightarrow 2[2],\quad \text{(ii) } [4]\rightarrow[3]+[1]\ ,\quad \text{(iii) } [4]\rightarrow 4[1]\ . \tag{6.3}$$

An examination of the simple chiral clock model with Hamiltonian (2.1) for general p indicates that at low temperatures the actual transition of a q wall as $\Delta>0$ increases will be into q distinct walls separated by $q-1$ intruding layers or

$$[q]\rightarrow q[1]\quad (\Delta>0,\ 2\leq q\leq p-1)\ , \tag{6.4}$$

yielding the relation $\Sigma_q=q\Sigma_1$ *at* and beyond the transition (see further below). However, we cannot rule out the possibility that, at sufficiently high temperatures, entropy effects might, for example, stabilize a [2] wall, and so allow the transition $[3]\rightarrow[2]+[1]$ to occur *before* the transition $[2]\rightarrow 2[1]$. Indeed, if the cosine function in (2.1) is replaced by a more general coupling form one can arrange that such "inversions" will occur. Nonetheless it is reasonable to expect that the normal transition for a $[q]$ wall will correspond to transformation into "elementary" or most stable walls which for $\Delta \gtrless 0$ will be the walls $[+1]\equiv[+]$ and $[-1]\equiv[-]$, respectively, with tensions $\Sigma_1\equiv\Sigma_+$ and $\Sigma_{p-1}\equiv\Sigma_{-1}\equiv\Sigma_-$.

C. Wetting near the melting line

Now consider the approach from within the commensurate phase to the melting line, $T_M(\Delta)$, in a region where the transition is continuous and of positive chiral character $(\Delta>0)$. Since all differences between distinct domains must vanish at the transition, the elementary wall tension, $\Sigma_+(T,\vec{\Delta};\theta)$ must also go to zero. If ν is the appropriate, chiral exponent for the divergence of the correlation length, hyperscaling arguments (see Sec. III above) indicate $\Sigma_+ \sim t^{\mu}$ with $\mu=(d-1)\nu$ for $d\leq 4$, so that Σ_+ vanishes continuously as $t\propto[T-T_M(\Delta)]\rightarrow 0$. On the other hand, consider a $[q>1]$ wall which, by hypothesis, has *not* suffered a wetting transition as $t\rightarrow 0$.[28,37] This is clearly *less* favored by the chiral field and hence, one might argue, its tension would tend to vanish only at some larger T or Δ; but this is a contradiction since the wetting condition $\Sigma_q=q\Sigma_+$ would necessarily have been encountered *before* the melting line was reached. This argument, which is at best heuristic, thus suggests that *wetting transitions should have taken place in all but the elementary walls before any portion of chiral melting line is reached.*

Various consequences follow from this conclusion. First, since at $\Delta=0$ [or $\zeta=\zeta_0(T)$] chirality is absent, one has $\Sigma_q\equiv\Sigma_{-q}$ so that if the melting is still continuous, as it is for $p=3$ and $d=2$, the wetting transition $[p-1]\equiv[-1]\rightarrow(p-1)[1]$ will *not* take place until t vanishes. It follows that the corresponding wetting locus in the (T,Δ) plane must *meet* the melting boundary at the symmetric multicritical point $\Delta=0$, as illustrated in Fig. 5(c) (see also Refs. 28 and 37). We expect that the "higher-order" wetting lines for $p\geq 4$, corresponding to $[q]\rightarrow q[1]$ for $q=2,3,\ldots,$ will also meet the multicritical point. (See further below for possible exceptions.) To obtain the form of the wetting lines near the symmetric multicritical point, we may generalize (3.3) to obtain the scaling hypothesis

$$\Sigma_q(T,\Delta;\theta)\approx\tilde{t}^{\mu}S_q(\Delta/\tilde{t}^{\phi};\theta)\ , \tag{6.5}$$

where the nonlinear thermal scaling field has the form

$$\tilde{t}=t-c_2\Delta^2+O(t^2,t\Delta^2,\Delta^4)\ . \tag{6.6}$$

The scaling functions $S_q(y;\theta)$ must all vanish at $y=\pm y_M$ on the commensurate phase boundary, given by $T=T_M(\Delta)$, or equivalently, by $\Delta=\Delta_M(T)$, which thus has the asymptotic form

$$\Delta_M(T)\approx\pm y_M\tilde{t}^{\phi}\ . \tag{6.7}$$

The wetting lines should have a similar form, namely,

$$\Delta_W^{(q)}(T;\theta)\approx y_W^{(q)}(\theta)\tilde{t}^{\phi}\ , \tag{6.8}$$

where $y_W^{(q)}$ is, in fact, the smallest value of the scaled variable y for which one has

$$S_q(y;\theta)=qS_1(y;\theta)\ . \tag{6.9}$$

It is worthwhile to consider the higher-order wetting lines in a little more detail. Consider a $[q]$ wall with $q\neq\pm 1 \pmod p$ in a *symmetric* clock model (i.e., *at* $\Delta=0$). The stability relation yields, in particular, $\Sigma_q\leq q\Sigma_+$ and $\Sigma_q\leq(p-q)\Sigma_-$. If either of these inequalities holds as an

equality we may presume that the $[q]$ wall is wet. One possibility is that the $[q]$ wall is always wet, even at $\Delta=0$, being decomposed into q elementary $[+]$ or $p-q$ elementary $[-]$ walls, depending on which configuration yields the lowest free energy. At low temperatures this is, in fact, the situation in the simple clock model with Hamiltonian (2.1); for $p=4$ this remains true at all temperatures and we suspect this also occurs for $p>4$. When this is the situation there are, physically, really only two types of wall, namely, $[+]$ walls and $[-]$ walls. The basic transition that takes place in a $[q]$ wall when Δ increases from negative values is then really a *wet-to-wet transition* described by

$$[q]\equiv(p-q)[-]\rightarrow q[+]\,. \tag{6.10}$$

The associated transition line is determined by $(p-q)\Sigma_-(T,\vec{\Delta};\theta)=q\Sigma_+(T,\vec{\Delta};\theta)$ and so, by the previous arguments, it will certainly run to the multicritical point at $\Delta=0$ in accord with (6.8). Notice that when p is even, a $[\frac{1}{2}p]$ wall at $\Delta=0$ can, by symmetry, have a structure corresponding either to $\frac{1}{2}p\,[+]$ walls or to $\frac{1}{2}p\,[-]$ walls: it follows that the wetting line for the transition $[\frac{1}{2}p]\equiv\frac{1}{2}p[-]\rightarrow\frac{1}{2}p[+]$ in such a wall coincides with the $\Delta=0$ axis.

On the other hand, it is possible that some of the $[q\neq\pm1]$ walls become intrinsically stable at higher temperatures for $\Delta=0$ in the simple clock model or, if the cosine coupling in (2.1) is suitably generalized, even at $T=0$. This stability might persist up to the multicritical point or wetting might occur at some intermediate temperature. A variety of increasingly elaborate wetting phase diagrams can thus be imagined and most are probably realizable in appropriately extended models. We examine some possibilities at the end of this section.

D. Nature of chiral melting

Our conclusion regarding the necessity of all walls undergoing wetting transitions as the chiral melting boundary is approached is also relevant to the question "what is the nature of the chiral melting transition, and, in particular, how does it differ from symmetric clock melting?" In the vicinity of the chiral melting line any wall of significant length must be an elementary, say a $[+]$ wall. Now the diverging critical fluctuations that characterize a continuous commensurate melting transition (chiral or nonchiral) may be envisaged[37] as microscopic heterodomains, i.e., subdomains of wrong phase within an otherwise uniform domain (with, otherwise, only relatively small deviations of adsorbate atoms from their ideal sites, etc.) as illustrated in Fig. 7. Consider now, for concreteness, a uniaxial $p=3$ surface phase. For a given total length of wall in the symmetric or neutral limit ($\Delta=0$, $\zeta=\zeta_0$) where $\Sigma_+=\Sigma_-$, the boundaries of the most probable domains will form simple loops enclosing one of the $p-1$ heterophases, even though, as illustrated in Fig. 7(a), there will, statistically, be some two-loop or compound subdomains in which two or more distinct heterophase regions share a boundary.

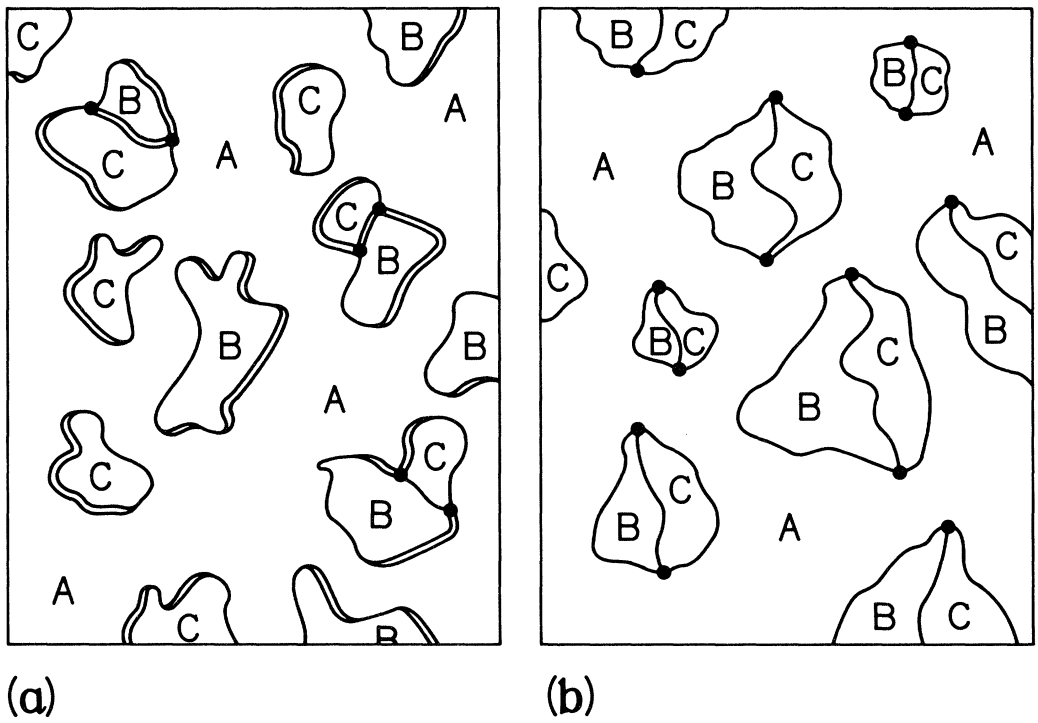

FIG. 7. An illustration of the dominant types of fluctuation near melting of the commensurate phase of the three-state chiral clock model for $d=2$, or, more generally, of a 3×1 uniaxial surface phase. For $\Delta=0$, i.e., on the locus $\zeta=\zeta_0(T)$ of effective symmetry, the fluctuations involve both $[-]$ walls (double lines) and $[+]$ walls (single lines) as shown in (a); off the symmetry locus, with $\Delta>0$, only $[+]$ walls may, asymptotically, occur as in (b) so that single-loop subdomains are suppressed.

In a chiral region, however, one side of each single-loop microdomain will represent an unfavored wall with tension $\Sigma_- > \Sigma_+$ (shown as a double line in Fig. 7). Upon crossing the wetting transition any such subdomains of large size will thus decompose into compound, two-loop form with only elementary walls, as shown schematically in Fig. 7(b). Notice, by the same token, that only chirally favored two-loop subdomains, say of $A(B \mid C)A$ character, will be present asymptotically for $\Delta > 0$, whereas in the neutral, $\Delta = 0$ case the opposite, $A(C \mid B)A$, subdomains will appear with equal frequency. This picture of the drastically different nature of the dominant critical fluctuations driving the melting transition in the two cases provides a direct answer to our question: It seems most unlikely that the symmetric, Potts melting exponents can be preserved in the chiral regime. Similar arguments apply for the uniaxial case with $p > 3$.

It is much harder to answer the question: "In which direction do the exponents change?" The crude approximation of regarding the critical fluctuations as described by an ideal gas of (noninteracting) microdomains leads to the suggestion that the chiral specific-heat exponent, α, should be smaller (i.e., less positive) than for the symmetric model, essentially because the two-loop domains have relatively less entropy because of the constraint that both loops must close (see also below). However, such a conclusion must remain highly speculative as regards the critical behavior.

In the next two sections we examine the transitions between uniaxially commensurate phases and the associated uniaxial or "striped" incommensurate phases using, as in previous studies,[5,42,43] the approximation that the system may be described simply as a collection of fluctuating domain walls, with only one class of domain walls, the [+] walls, allowed. The wetting transitions described above help justify this approximation; since long segments of the other classes of domain wall will not occur beyond the wetting transitions, they cannot play an important role in the critical phenomena.

Similar arguments regarding the stability of various sorts of domain wall can be brought to bear in triaxially chiral Potts models and hexagonal commensurate $\sqrt{3}\times\sqrt{3}$ surface phases and should play a role in the crossover from Potts to chiral universality classes that occurs at the postulated multicritical point M in the phase diagram of Fig. 4. Thus, on the Potts section of the melting line the tensions $\Sigma_+(T,\zeta)$ and $\Sigma_-(T,\zeta)$ should approach one another asymptotically with $\Sigma_+/\Sigma_- \to 1$. In the vicinity of M, contours of constant Σ_+/Σ_- should represent scaling loci converging on M, mirroring those shown in Fig. 4 as dotted curves in the disordered region. Such considerations might also serve to justify the approximation of allowing only one class of wall in the study of the incommensurate-commensurate transition in hexagonal phases as initiated by Villain[66] and developed by Coppersmith *et al.*[5] However, in a $\sqrt{3}\times\sqrt{3}R30°$ commensurate phase a [+] wall in a given natural orientation becomes a [−] wall on rotation through 60°, and vice versa; this can be verified with the aid of Fig. 3. By contrast, a rotation of 180° is needed to effect this interchange in a uniaxial $p\times 1$ system. This fact complicates the analysis of the way in which walls in a hexagonal phase may transform under variation of T and Δ. For this reason we defer discussion of hexagonal phases until another occasion.

E. Nature of the wetting transition in two dimensions

It is clearly of interest to understand the nature of the basic wall wetting transition illustrated in Fig. 6. Answers in closed form for the chiral clock or similar models seem unattainable although, as mentioned, some progress can be made analytically at low temperatures for the $p=3$ chiral clock model.[28] However, a more or less complete analysis can be made for two-dimensional systems on a semiphenomenological basis[5,42] in which a wall segment is regarded as a random walker diffusing along the x axis (i.e., in a direction parallel to the chiral field, $\vec{\Delta}$) but which proceeds "forward" in the timelike, y-axis direction. Within this approach the theory of the wetting transition represented in Fig. 6 is completely analogous to theoretical treatments of the denaturation of a double-stranded biopolymer such as deoxyribose nucleic acid (DNA).[67]

To develop the theory (see also Ref. 28) let us introduce the Boltzmann weights

$$w_\pm = \exp(-\bar{\sigma}_\pm) \quad \text{with } \bar{\sigma}_\pm = \sigma_\pm / k_B T \,, \tag{6.11}$$

for a unit length of [+] or [−] wall projected on to the y axis, where $\sigma_+(T,\Delta)$ and $\sigma_-(T,\Delta)$ represent the semimicroscopic, "intrinsic" or "fluctuationless" wall tensions which vary smoothly with T and Δ. In renormalization-group language, σ_+ and σ_- would be the microscopic tensions renormalized to the chosen "unit" length scale. A single strand of length n of, say, [−] wall (see Fig. 6) has a Boltzmann factor w_-^n and, hence is described by a generating function (or propagator)

$$\mathcal{G}_1(w_-;x) = 1/(1-w_- x) \,, \tag{6.12}$$

in the expansion of which the coefficient of x^n represents the weight of all wall configurations of length n or, in walk language, of all n-step random walks. There will, similarly, be a generating function $\mathcal{G}_2(w_+;x)$ that describes the "bubbles" or double strands of [+] wall which start at a common junction point and meet again n steps later *without* having crossed in the meanwhile. If we consider the more general wetting transition (6.4) in which a [q] wall dissociates into q [+] walls, the simple bubbles in Fig. 6(a) should be replaced by "bananas" (or "watermelons") of q-fold strands as shown in Fig. 6(c) for $q=3$. There will be a corresponding generating function,

$$\mathcal{G}_q(w_+,x) = \sum_{n=1}^{\infty} g_n^{(q)} w_+^{ng} x^n \,, \tag{6.13}$$

in which $g_n^{(q)}$ measures the probability that q walkers who start together proceed to walk without meeting or crossing paths until they finally all reunite together on their nth step.

Note that the *junctions* between single-stranded sections of wall and double- (or q-fold)-stranded sections will have a distinct microscopic structure and an associated excess free energy which may be accounted for by introducing an

activity, z, for each junction. [When $q=(p-1)$ we will, in Sec. VII below, identify the "junctions" as *dislocations* in the configuration of the local order parameter defined via $\psi_r=\exp(2\pi i n_r/p)$.] The generating function for the "full" or "dressed" $[-]$ or, more generally, $[q]$ wall is then given by[28,67]

$$\mathscr{G}(w_+,w_-;x)=\frac{\mathscr{G}_1(w_-;x)+\mathscr{G}_q(w_+;x)}{1-z^2\mathscr{G}_1(w_-;x)\mathscr{G}_q(w_+;x)}. \quad (6.14)$$

The desired full domain-wall tension, $\Sigma_q(w_+,w_-)$, is then determined via

$$\exp[\Sigma_q(w_+,w_-)/k_BT]=x_0(w_+,w_-)\ , \quad (6.15)$$

where x_0 is the nearest (necessarily, real) singularity of $\mathscr{G}(x)$ which lies closest to the origin $x=0$. Evidently x_0 represents the radius of expansion of the series for $\mathscr{G}$ in powers of x.

Now x_0 is determined either, using (6.12), by the *exterior condition,*

$$1-w_-x=z^2\mathscr{G}_q(w_+;x)\ , \quad (6.16)$$

corresponding to the vanishing of the denominator in (6.14), *or* by the nearest real, positive singularity x_q, of $\mathscr{G}_q(w_+;x)$, provided this generating function approaches a *finite* limit as $x\to x_q-$. It is not hard to conclude from (6.13) that $x_q=w_+^{-q}$ so that the *interior condition* is

$$x_0(w_+,w_-)=w_+^{-q}\ . \quad (6.17)$$

(See also Appendix A.) Via (6.15) this yields $\Sigma_q=q\sigma_+$; it follows that the interior condition describes the *wet* phase where $[q]$ has decomposed into q $[+]$ walls with individual tensions $\Sigma_+\equiv\sigma_+$. (This oversimple expression for Σ_+ clearly results from failure to include fluctuations in the structure of a $[+]$ wall; however, since the $[+]$ wall will not, *itself,* undergo a major structural change at the wetting transition, its singularities at this transition should be weaker than those in the $[q]$ wall.)

To decide *if* a wetting transition occurs or its character, if one does occur, it is necessary to know the singularity in the q-walker generating function at x_q. This problem, which turns out to be central for many applications of the domain-wall–random-walk theory is solved in Appendix A. As $xw^q\to 1-$ we find

$$\mathscr{G}_q(w,x)\approx\begin{cases}G_s/(1-xw^q)^{(3-q^2)/2}, & q<\sqrt{3}\\ G_s\ln(1-xw^q)^{-1}, & q=\sqrt{3}\\ G_c-G_s(1-xw^q)^{(q^2-3)/2}, & \sqrt{3}<q<\sqrt{5}\end{cases}, \quad (6.18)$$

and, for $q>\sqrt{5}$ but q^2 not an odd integer,

$$\mathscr{G}_q(w,x)\approx G_c-G_1(1-xw^q)+G_2(1-xw^q)^2+\cdots -G_s(1-xw^q)^{(q^2-3)/2}+\cdots\ , \quad (6.19)$$

where the positive coefficients G_s, G_c, G_1, etc., depend on q. When q^2 is an odd integer a factor $\ln(1-xw^q)^{-1}$ appears in the G_s term.

In using these expressions in the exterior condition (6.16) it is appropriate to regard w_- as the control variable which *decreases* as T and Δ increase. Then, considering continuous q for generality, we see that there is no transition for $q\le\sqrt{3}$; this correctly recaptures the absence of a transition in a single strand of alternating character. For $q>\sqrt{3}$, however, a sharp transition always occurs at

$$w_-=w_c(w_+)=w_+^q(1-z^2G_c)\ . \quad (6.20)$$

If we put

$$\hat{t}=w_--w_c(w_+)\sim T_W(\Delta)-T\ , \quad (6.21)$$

we find this transition is described by

$$\Sigma_q(T,\Delta)-q\Sigma_+(T,\Delta)\equiv 0,\ \ \hat{t}\le 0\ , \quad (6.22)$$

and, as $\hat{t}\to 0+$ (with $z\neq 0$), by

$$\Sigma_q-q\Sigma_+\approx -A_s\hat{t}^{2/(q^2-3)},\ \ q<\sqrt{5}\ ,$$
$$\approx -A_1\hat{t}+A_s\hat{t}^{(q^2-3)/2}+A_2\hat{t}^2+\cdots,\ \ q>\sqrt{5}\ , \quad (6.23)$$

where A_s can be expressed in terms of z, G_c, q, etc., and the A_s term gains a factor $(\ln\hat{t})^{-1}$ when q^2 is an odd integer [so that $k=(q^2-3)/2$ is an integer]. Evidently the transition is *continuous* for $q<\sqrt{5}$ and, in particular, for $q=2$ which corresponds to the basic wetting transition $[-]\to 2[+]$ in a $p=3$ system. The critical exponent for the domain-wall tension or interfacial free energy may be written

$$2-\alpha_W=2,\ \ p=3\ , \quad (6.24)$$

and evidently corresponds precisely to a classical, Ehrenfest second-order transition.[28,37] This result is also in concordance with Abraham's[68] exact calculation for an analogous wetting transition at a *rigid* wall in a two-dimensional Ising model. Our approach can be adapted in a straightforward way to the rigid-wall problem and yields the same results for exponents since the appropriate generating function for a bubble "stuck" on a wall has the same form as given by (6.18) with $q=2$. (This provides yet another heuristic derivation[69–72] of Abraham's exact result.) The agreement with the exact exponent values encourages us to believe that, as regards universal features such as exponent values, our result for general q will be correct for the chiral clock and similar models.

On returning to (6.23) we see that the wetting transition is of *first order* for $q>\sqrt{5}$ and hence for the basic transition $[-]\to(p-1)[+]$ in a p-state system with $p\ge 4$. There are, however, singular corrections at the first-order transition which, for integral q, take the form $\hat{t}^{k+1/2}$ or $\hat{t}^k/\ln\hat{t}$ (with k an integer).

It is of interest to enquire after further properties of a $[q]$ wall near its transition. To this end notice that $\mathscr{G}_q(w_+,x)$ is essentially a partition function for bubbles (or q-fold bananas). It follows that the *mean length* of a bubble (or banana) is given by

$$\langle n^{(q)}\rangle=\frac{\partial}{\partial x}\ln\mathscr{G}_q(w_+,x)\ . \quad (6.25)$$

On using (6.15), (6.19), and (6.23) one finds that $\langle n^{(q)}\rangle$

remains bounded for $q^2>5$, where the transition is first order, but diverges as

$$\langle n^{(q)}\rangle \sim 1/\hat{t}^{(5-q^2)/(q^2-3)}, \tag{6.26}$$

when $\hat{t}\to 0$ for $3<q^2<5$. For the case $q=2$ (or $p=3$) this yields $\langle n^{(q)}\rangle \sim \hat{t}^{-1}$ as the critical wetting transition is approached. A similar calculation using $\mathscr{G}_1(w_-,x)$ shows that the mean length of the single-stranded sections remains bounded right up to the transition, as might have been guessed.

Owing to the fluctuations, the *width* of a wall should diverge on approaching criticality. Now, because of the diffusive, random-walk character of a bubble, the mean width, $\bar{m}_n$, measured normal to the wall should vary as $n^{1/2}$ for large n. However, to calculate the mean width of the wall itself each bubble must be weighted by its own length n. Upon recalling (6.13) we can thus write the mean-wall width as

$$\langle m_\Sigma^{(q)}\rangle \approx \frac{\sum_n n^{3/2} g_n w_+^{nq} x^n}{\sum_n n g_n w_+^{nq} x^n}. \tag{6.27}$$

The denominator can be calculated, as in (6.25), by taking a first derivative of $\mathscr{G}_q(w_+;x)$ with respect to x. The numerator essentially requires a three-halves derivative but may be calculated alternatively by noting that the results (6.18) and (6.19) actually imply [and, conversely, follow from (see Appendix A) the asymptotic result

$$g_n \approx g_0/n^{(q^2-1)/2} \quad (n\to\infty). \tag{6.28}$$

Using this in (6.27) and estimating the sums asymptotically as $w_+^q x\to 1-$ yields

$$\langle m_\Sigma^{(q)}\rangle \sim 1/(q\Sigma_+-\Sigma_q)^{1/2} \sim 1/\hat{t}^{1/(q^2-3)}, \tag{6.29}$$

for $q^2<5$, where the transition is continuous. For $q=2$ ($p=3$) the width and, hence, the adsorption of the intermediate phase[48,73] on the wall, diverges simply as $1/\hat{t}$. (See also Ref. 28 for a more explicit calculation.) For $q^2>6$ the width of the $[q]$ wall remains finite at the transition as would be expected. (In the unphysical region $5<q^2<6$, the transition is of first order but $\langle m_\Sigma^{(q)}\rangle$ *still* diverges. This is just a reflection of the singular fluctuations still present near the transition.)

Finally, one may estimate the longitudinal wall correlation length $\xi_{\|}^{\Sigma}(T,\Delta)$, for correlations measured along the length of the wall, and the transverse correlation length, $\xi_{\perp}^{\Sigma}(T,\Delta)$, describing correlations across the width of the wall, by the same methods. (Note that these wall correlation lengths are *distinct* from the corresponding correlation lengths $\xi_{\|}$ and $\xi_{\perp}$ observable in the bulk of a domain; see the following sections.) Within a bubble of length n the correlations are locally of magnitude n parallel to the wall but, appealing to the diffusive character, of order $n^{1/2}$ across the wall. However, the probability that a given point near a wall is actually within a bubble of length n is proportional to n. It follows that the transverse correlation length, $\xi_{\perp}^{\Sigma}$, is given by the same weighting expression (6.27) as yields the wall width (which might be anticipated on general grounds). For $\xi_{\|}^{\Sigma}$ the factor $n^{3/2}$ in the numerator of (6.27) is to be replaced by n^2. For $q^2<5$ we thus obtain

$$\xi_{\|}^{\Sigma} \approx (\xi_{\perp}^{\Sigma})^2 \sim \langle m_\Sigma\rangle^2 \sim 1/(q\Sigma_+-\Sigma_q). \tag{6.30}$$

Finally, for the practical case $q=2$ ($p=3$) we obtain

$$\nu_W^{\|}=2, \quad \nu_W^{\perp}=1. \tag{6.31}$$

Note that the result for $\nu_W^{\|}$ agrees via hyperscaling for a $(d=1)$-dimensional system (i.e., a wall) with (6.24). The result for $\nu_W^{\perp}$ is the same as the analogous exact result found by Abraham[68] for the wetting transition at a rigid wall in the two-dimensional Ising model, again confirming the validity of the simple random-walk approach.

F. Wet to wet transitions

As explained above, the basic wall transition in a uniaxial system with $p\geq 4$ should be described by (6.10) in which a $[q]$ wall with $2\leq q\leq p-2$ decomposes either into $(p-q)$ $[-]$ walls or transforms into q $[+]$ walls. However, there remains the possibility that a q wall can, for some T and Δ, have a coherent, "bound" or "dry" structure with fluctuations consisting of alternating q-stranded bananas of $[+]$ walls and $(p-q)$-stranded bananas of $[-]$ walls. One might wish to allow also sections of microscopically intrinsic $[q]$ wall: These can be accounted for by generalizing the junction activity, z, to a renormalized activity $\tilde{z}=z\mathscr{G}_1(w_q;x)$. This modification will, however, not affect the main qualitative results so we shall ignore it here. The appropriate generating function for a $[q]$ wall is thus obtained from (6.14) merely by replacing $\mathscr{G}_1(w_-;x)$ by $\mathscr{G}_{p-q}(w_-;x)$.

There are then two separate *interior conditions,* namely, $x_0 w_+^q=1$ as before, and $x_0 w_-^{p-q}=1$, where the smallest value of x_0 must be chosen. These solutions evidently describe the two distinct wet regimes: one with only $[+]$ walls in which $\Sigma_q=q\Sigma_+=q\sigma_+$ and one with only $[-]$ walls in which $\Sigma_q=(p-q)\Sigma_-=(p-q)\sigma_-$. On the other hand, the smallest singularity may arise from the *exterior condition*

$$z^2\mathscr{G}_{p-q}(w_-;x_0)\mathscr{G}_q(w_+;x_0)=1, \tag{6.32}$$

which describes a coherent wall structure which might exist in a *dry* region of the phase diagram.

There are clearly two relevant parameters in the problem, say,

$$\bar{\Delta}=\ln(w_+^q/w_-^{p-q})=(p-q)\sigma_- - q\sigma_+, \tag{6.33}$$

which, loosely, may be regarded as corresponding to Δ or ζ, and the activity z which, again loosely, may be regarded as increasing with the temperature T. Following the previous analysis one sees, first, that for $q<\sqrt{3}$ and $p-q<\sqrt{3}$ only a coherent wall or dry phase is possible. Conversely, the $[+]$ and $[-]$ wet phases exist only for $q>\sqrt{3}$ and $(p-q)>\sqrt{3}$, respectively. The coherent-to-dissociated, $[+]$ walls or dry—to—$[+]$-wet transition is again continuous with exponent $2-\alpha_W=2/(q^2-3)$ for $q<\sqrt{5}$ and first order for $q\geq\sqrt{5}$ with correction exponent $\theta_W=\frac{1}{2}(q^2-3)$; likewise for the dry—to—$[-]$-wet transitions. When both q and $(p-q)$ exceed $\sqrt{3}$ there is

either a bicritical point, a critical endpoint, or a triple point at

$$\bar{\Delta}=0,\quad z_0=[G_c^{(p-q)}G_c^{(q)}]^{-1/2}\,, \tag{6.34}$$

using the critical values defined in (6.18) and (6.19). For $z<z_0$ there is always a simple first-order wet-to-wet transition on the $\bar{\Delta}=0$ axis (with no singular corrections). The dry phase or coherent regime exists only above z_0. The possible phase diagrams in the vicinity of the multiphase point for realistic (i.e., integral) values of p and q are illustrated in Fig. 8. In the bicritical case (a) $p=4$ and $q=2$, the critical lines depart quadratically from the $\bar{\Delta}=0$ axis; in (b) there is a discontinuity in the curvature of the first-order boundary at the critical endpoint.

The possibility of stabilizing a coherent higher-order wall revealed by these figures was alluded to previously. One may reasonably doubt, however, if the appropriate junction activity, z, can ever become sufficiently large in the simple clock models to realize such regimes. Nevertheless, this feature could well arise in more complex models or real systems.

VII. COMMENSURATE-INCOMMENSURATE TRANSITIONS

In this section we reexamine the random-walk or "wall-wandering" model for the transition between commensurate and uniaxial or "striped" incommensurate phases[5,14] as expounded by Fisher and Fisher,[42,74] in order to obtain various further critical exponents. The need to consider *dislocations* is discussed.

In the wall-wandering picture the incommensurate phase is assumed to consist simply of more or less parallel domain walls that may fluctuate in relative position. When the system has dimensionality $d<3$ the dominant interaction between the walls at large average wall separations (as relevant near the transition) arises from the reduction of each wall's freedom to fluctuate caused by collisions with the other walls. (It is appropriate to assume an effective "hard-core" repulsion between walls.) If the average wall separation is l, one may estimate[42] the number of collisions per unit $(d-1)$-dimensional "area" of a single wall as

$$A_0/A_l\approx B_d(b_\perp/l)^{2(d-1)/(3-d)}\quad(1<d<3)\,, \tag{7.1}$$

where B_d is a numerical coefficient, $A_0=b_{||}^{d-1}$ is a suitable reference area, while the scale $b_\perp$ which represents the diffusivity or elasticity of the wall is set by

$$b_\perp^2(T)=c_d k_B T/\tilde{\Sigma}(T)b_{||}^{d-3}\,, \tag{7.2}$$

in which $\tilde{\Sigma}(T)$ represents the *wall stiffness*.[42,75] By choosing A_0 so that each collision reduces the wandering entropy of a wall by an amount k_B one obtains[42,74(b)] an expression for an effective wall-wall interaction potential which decays with wall separation as $l^{-\tau}$ where

$$\tau=2(d-1)/(3-d)\,, \tag{7.3}$$

yielding $1/l^2$ for $d=2$.

The thermal fluctuations of the walls give the incommensurate phase the character of an elastic medium and lead, for $1<d<3$, to correlations in the local order parameter,

$$\psi(\vec{r})=\exp[2\pi i\bar{n}(\vec{r})/p]\,, \tag{7.4}$$

which decay algebraically with distance, $|\vec{r}|$; for $d>2$ there is also long-range order present. [Compare this definition of the order parameter with (3.16); here $\bar{n}(\vec{r})$

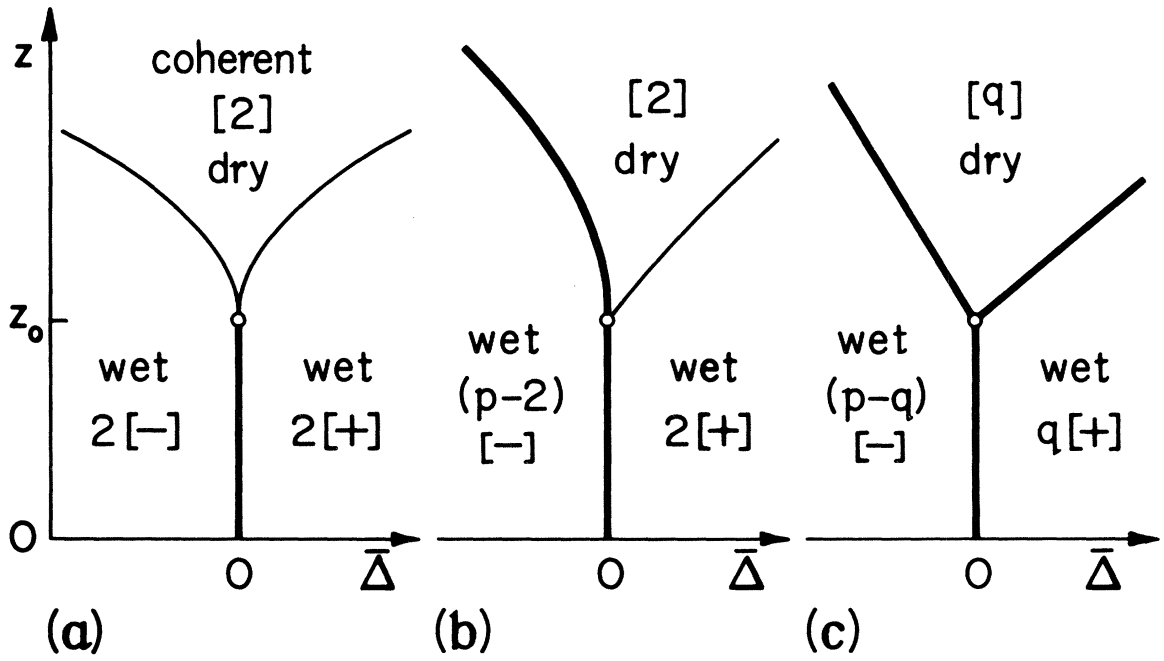

FIG. 8. Phase diagrams for *wet-to-wet* domain-wall transitions in two-dimensional uniaxial systems for a [2] wall in a system with (a) $p=4$ and (b) $p\geq 5$, and (c) for $[q\geq 3]$ walls with $p-q\geq 3$. Bold lines denote first-order transitions; classical second-order transitions are shown by light lines. A single coherent wall, or dry regime, exists only for $z>z_0$.

represents a local but coarse-grained value of the p-state clock variables.] The wall fluctuations, however, are limited by the presence of the adjacent walls and the lengths characterizing these limits may be viewed as correlation lengths setting the scales *beyond* which the algebraic decay laws become asymptotically exact. These correlation lengths will, in fact, diverge as the incommensurate-commensurate transition is approached. (We assume the *C-I* transition is continuous here.) Normal to the walls, the length limiting the fluctuations is clearly just the average wall separation, l. This in turn determines the *incommensurability*, $\bar{q}=\langle d(\arg\psi)/dx\rangle$ which vanishes at the transition. Thus we may write

$$l=2\pi/p\bar{q}(T,\xi)\approx\xi_\perp \ . \tag{7.5}$$

Likewise the average spatial separation between neighboring wall collisions sets the scale of the correlations parallel to the wall so that, by (7.1), we can conclude

$$\xi_{||}\sim l^{2/(3-d)}\sim\xi_\perp^{2/(3-d)} \ . \tag{7.6}$$

For $d=2$ this yields $\xi_{||}\sim\xi_\perp^2$ which is reminiscent of the results of the last section for the correlation lengths, $\xi_{||}^\Sigma$ and $\xi_\perp^\Sigma$, within a single wall in the commensurate phase: Note, however, that we are here discussing correlation lengths which characterize the *bulk* incommensurate phase.

In the commensurate phase, the domain-wall tension, $\Sigma(T,\xi)$, is positive and walls do not spontaneously appear. However, as the commensurate-incommensurate transition boundary, say $\xi_{CI}(T)$ or $\Delta_{CI}(T)$, is approached this wall tension vanishes. Following Ref. 42 we assume $\Sigma(T,\xi)$ varies smoothly through the transition and thus write

$$\Sigma=-\sigma'\delta \ \text{ with } \delta\approx\xi-\xi_{CI}(T)\sim\Delta-\Delta_{CI}(T) \ . \tag{7.7}$$

We will, here, also add a p-component field, $\vec{h}$, that couples separately to each of the p different domains (see more explicitly below). This field will be supposed infinitesimally small so that it has negligible effect on the fluctuations of the walls. Now we construct[42] the free-energy density in terms of the mean wall separations but we allow different wall separations, l_k, for the p different domains, the overall mean wall separation, l, then satisfying

$$pl=\sum_{k=0}^{p-1} l_k \ . \tag{7.8}$$

The free-energy density functional consists[42] of a sum of terms arising from the wall tension, the wall-wall interactions, and the field $\vec{h}$, namely,

$$\mathcal{F}(\delta,\vec{h};\{l\})\approx-\frac{\sigma'\delta}{l}+\frac{\tilde{B}}{pl}\sum_{k=0}^{p-1} l_k^{-\tau}-\frac{1}{pl}\sum_{k=0}^{p-1} h_k l_k \ , \tag{7.9}$$

where $\tilde{B}=k_BTA_0B_db_{||}^\tau$. As indicated, this expression is valid for dimensionalities in the range $1<d<3$.[42]

The system will choose the configuration of minimal free-energy density. For the incommensurate phase δ is positive (by definition) and it is then convenient to write

$$\bar{l}_i=(\sigma'\delta/\tilde{B})^{1/\tau}l_i \ \text{ and } 1+\tau^{-1}=\tau' \ , \tag{7.10}$$

so that the free-energy density becomes

$$f(\delta,\vec{h})\approx\tilde{B}\left[\frac{\sigma'\delta}{\tilde{B}}\right]^{\tau'} \times\min_{\{l_i\}}\left[\frac{1}{p\bar{l}}\sum_{k=0}^{p-1}\left[\frac{1}{\bar{l}_k^\tau}-\frac{\tilde{B}^{1/\tau}h_k\bar{l}_k}{(\sigma'\delta)^{\tau'}}\right]-\frac{1}{\bar{l}}\right] . \tag{7.11}$$

This shows that the free energy has the scaling form

$$f(\delta,\vec{h})\approx|\delta|^{2-\alpha}Y_\pm(\vec{h}/|\delta|^\Delta) \tag{7.12}$$

with exponents

$$2-\alpha=\Delta=1+\tau^{-1}=(d+1)/2(d-1) \ , \tag{7.13}$$

which give $\alpha=\frac{1}{2}$ and $\Delta=1\frac{1}{2}$ for $d=2$.

In this description the commensurate phase of the system is inert, being composed of a single domain of infinite width; the free-energy density is simply $f=-\max_k\{h_k\}=-h_j$ where j determines the nature of the domain present. The order parameter $\psi(\vec{r})$ is constant throughout the domain and the susceptibility and all fluctuations vanish identically. This cannot be a fully realistic description but we will return to this point shortly.

In the incommensurate phase, at $\delta>0$, the zero-field critical behavior of the commensurate-incommensurate transition follows directly. The susceptibility for the field $\vec{h}$ diverges as[74(c)]

$$\chi\sim\delta^{-\gamma} \ \text{ with } \gamma=(d+1)/2(d-1) \ . \tag{7.14}$$

The incommensurability vanishes as[42]

$$\bar{q}(\delta)\sim\delta^{\bar{\beta}} \ \text{ with } \bar{\beta}=(3-d)/2(d-1) \ , \tag{7.15}$$

so that

$$l\approx\xi_\perp\sim\delta^{-\nu^\perp} \ \text{ with } \nu^\perp=\bar{\beta} \ , \tag{7.16}$$

while the longitudinal correlation length diverges as

$$\xi_{||}\sim\delta^{-\nu^{||}} \ \text{ with } \nu^{||}=1/(d-1) \ . \tag{7.17}$$

Note that the bulk hyperscaling relation for anisotropic scaling is obeyed, namely,

$$2-\alpha=\nu^\perp+(d-1)\nu^{||} \ . \tag{7.18}$$

The results for $\bar{\beta}=\nu^\perp$ and for $\nu^{||}$ in the case $d=2$ agree with the more microscopic analyses of Pokrovsky and Talapov[14] and Schulz.[76]

One reason for the inertness of the commensurate phase in the description presented is obvious: By *choice* we have adopted a *semi*microscopic (or *semi*macroscopic) viewpoint in which the properties of a uniform domain are treated as known and smoothly varying with intrinsic microscopic fluctuations purposely ignored. More significant from our present perspective, however, is that we have not allowed for the possible existence of *thermally excited dislocations* (or *vortices*).

Let us now focus attention explicitly on *two-dimensional systems.* We say a single *dislocation* is present in a given simply connected region if, on tracing a

path along the boundary of the region the phase of the order parameter, $\psi(\vec{r})$, as defined in (7.4), changes by 2π.[77] In terms of walls separating distinct domains this means the path must have crossed p elementary ($\Delta n = \pm 1$) walls and, hence, that a dislocation represents the junction of precisely p distinct walls.

It is worth stressing that because of the coarse graining or, at least, time averaging, needed to define an appropriate local order parameter, the existence of a dislocation in the sense described, i.e., a *semimicroscopic* or *order-parameter dislocation,* need *not* imply a corresponding dislocation or topological defect in the microscopic description in terms of a lattice of particles adsorbed on a substrate. In a $p \times 1$ phase, such as illustrated in Fig. 2, there will be such a correspondence in the case that all the walls closely correspond to the ideal heavy $A \mid B$ wall on the left of the figure. However as ζ varies across the commensurate phase and the presence of vacancies, etc., changes the nature of the wall, this strict correspondence will normally break down. We remark parenthetically that the situation is more complex in the case of hexagonal phases even if only ideal walls such as shown on the left of Fig. 3 are involved.[78]

It is clear that a consistent treatment at the domain-wall or random-walk level, must allow for the spontaneous creation of dislocations. A typical pair of dislocations, as might appear in the commensurate phase of a $p=4$ system are shown in Fig. 9. (Compare with Fig. 6.) The balance of our discussion in this and subsequent sections is devoted to the question of how such dislocations affect the commensurate-incommensurate transition in two dimensions. We will, in particular, show that allowing for such dislocations constitutes a *relevant* perturbation of the wall wandering description only for $p < \sqrt{6}$.

Note, however, that the model in which dislocations are strictly forbidden may be appropriate for modeling fluctuations in a simple face of a cubic crystal oriented near, say, a (100) orientation.[79] Such a crystal surface will consist of plateaus at different levels, relative to the precise (100) axis, separated by steps: The former may be regarded as domains, the latter as domain walls. Modeling the steps simply as fluctuating domain walls makes sense if each step consists of an addition of just one atomic layer and the steps repel one another. The field δ that now couples to the step free energy is conjugate to the orientational angle of the crystal face. A dislocation in the p-state model may arise because after crossing p walls one returns to the domain one started in. For a crystal face, however, one cannot ever leave and return to a given level simply by stepping upwards. Thus there can be no dislocations in the present sense on the face of a perfect crystal. (In an alternative view such a system may be regarded as realizing a $p \to \infty$ model.)

Dislocations play a role in the equilibration of an incommensurate phase similar to that of vortices in the decay of superfluid flow.[80] Indeed, domain walls may be added or removed from the system in a "continuous" fashion only by the nucleation and growing separation of dislocation pairs or by the annihilation of approaching pairs. Thus, as the dislocations illustrated in Fig. 10 separate, the upper one moving higher and lower one still lower, they leave behind $p=3$ new domain walls and hence change the mean separation of walls through the system and so may serve to bring the incommensurability $\bar{q}(T,\zeta)$ to its equilibrium value.

For $d=2$ and $\vec{h}=0$ the free-energy density (7.9) may be written as a function of the wall density or incommensurability, $\bar{q}$, as

$$\mathcal{F}(\delta;\bar{q}) \approx -(p\sigma'\delta/2\pi)\bar{q} + \bar{B}\bar{q}^3 , \tag{7.19}$$

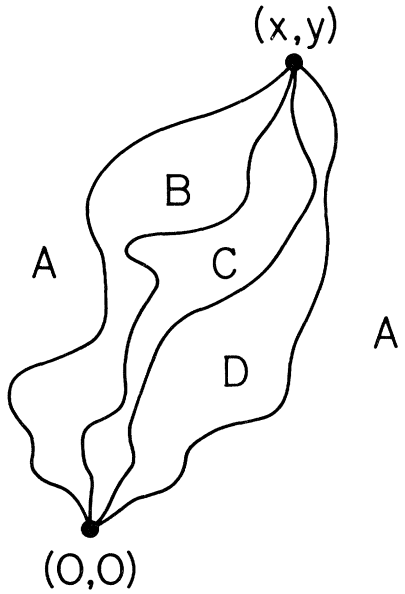

FIG. 9. Illustration of a configuration of a commensurate $p=4$ phase containing a pair of dislocations. Four (elementary) domain walls emanate from each dislocation. More generally, p elementary walls meet at each dislocation.

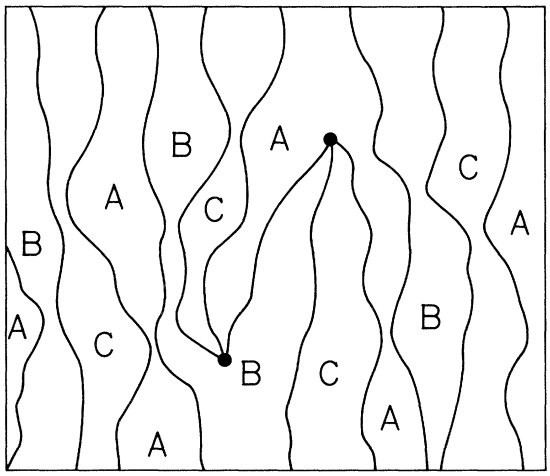

FIG. 10. Two dislocations in a uniaxial or striped weakly incommensurate $p=3$ phase. Domain walls separate, successively, A, B, and C domains and so on. Note that if the two dislocations approach they may mutually annihilate to leave only a regular, more or less parallel array of walls. Conversely, if their separation increases, in a vertical direction, one eventually obtains a state in which $p=3$ extra domain walls cross the system with consequent change in the incommensurability, $\bar{q}(T,\zeta)$.

with $\bar{B}=p^2\tilde{B}/8\pi^3$. Equilibrium will be established at the incommensurability

$$\bar{q}_0(\delta)\approx(p\sigma'\delta/6\pi^2\bar{B})^{1/2} . \tag{7.20}$$

If the actual, nonequilibrium incommensurability is $\bar{q}$ the extra free energy per unit length arising from adding a domain wall is

$$\frac{\partial\mathcal{F}}{\partial\bar{q}}\approx-(p\sigma'\delta/2\pi)+3\bar{B}\bar{q}^2\approx3\bar{B}(\bar{q}^2-\bar{q}_0^2) . \tag{7.21}$$

Now Schulz, Halperin, and Henley[43] have found that the excess free energy at equilibrium due to a dislocation pair in the incommensurate phase varies as the product of the temperature, $\frac{1}{2}p^2$ and the logarithm of the separation. Thus when two dislocations separate, moving parallel to the domain walls and introducing p new walls, the associated net excess free energy is given by

$$V(y)\approx2E_0+\tfrac{1}{2}k_BTp^2\ln y+3\bar{B}p(\bar{q}^2-\bar{q}_0^2)y \tag{7.22}$$

for longitudinal separation y, where E_0 represents dislocation core energy. When $\bar{q}<\bar{q}_0$ the dislocation pair must thus cross a nucleation barrier of height

$$V_{\max}=2E_0+\tfrac{1}{2}k_BTp^2[\ln(k_BTp/6\bar{B})-\ln(\bar{q}_0^2-\bar{q}^2)-1/p] \tag{7.23}$$

in order to introduce p new walls across the entire system, thereby *lowering* the total free energy and moving $\bar{q}$ towards the equilibrium value $\bar{q}_0$. The rate of such nucleation should be proportional to the Boltzmann factor $\exp(-\beta V_{\max})$. Consequently we expect that $\delta\bar{q}/\delta t$, the rate of approach to equilibrium, should vary as $R\,|\bar{q}_0^2-\bar{q}^2|^{p^2/2}$; however, the rate constant, R, which certainly depends on E_0, T, p and $\bar{B}$, will probably also entail a further factor $|\bar{q}_0^2-\bar{q}^2|^{\lambda}$ where λ is determined by the details of the nucleation process (but might not depend explicitly on p). Such a rate law leads to the decay of $\bar{q}(t)-\bar{q}_0$ as an inverse power, $1/t^{\omega_p}$ with $\omega_p=2/(p^2-2+2\lambda)$. For $p\geq3$ and if $\lambda\geq-1$ this yields $\omega_p<0.4$ so that rather slow decays are to be anticipated. This may well lead to observable hysteresis in some systems.

VIII. DISLOCATION INTERACTIONS IN TWO DIMENSIONS

Let us now consider the theory of the transition from a uniaxial commensurate phase to the corresponding striped incommensurate phase in two dimensions with dislocations allowed. If, as in Sec. VI, the dislocation activity or fugacity is z, the singular part of the free-energy density in zero field should scale for small z and $|\delta|$ as

$$f_s\approx|\delta|^{3/2}W_{\pm}(z/|\delta|^{-\theta_p}) , \tag{8.1}$$

where the crossover exponent for dislocations in a p-state system has been called $-\theta_p$. The dislocations represent *relevant* perturbations at the $\delta=0$ transition point if $\theta_p<0$; conversely, if θ_p is positive only singular corrections to scaling are implied. Assuming that the scaling functions, $W_{\pm}(w)$, are analytic at the origin, we may expand as

$$f_s=|\delta|^{3/2}W_{\pm}(0)+|\delta|^{\theta_p+3/2}zW'_{\pm}(0)+\tfrac{1}{2}|\delta|^{2\theta_p+3/2}z^2W''_{\pm}(0)+\cdots . \tag{8.2}$$

Note that inside the incommensurate phase the dislocations are known[5,19] to be relevant when $p^2<8$: Furthermore, because of the algebraic decay of correlations within that phase when $z=0$ the corresponding scaling function might well be singular at $w=0$ so that a simple Taylor expansion might not be justified. However, we will make use of the expansion only in the commensurate phase ($\delta<0$), where it should be well behaved. As shown in the preceding section, the singular part of the free energy in the commensurate phase vanishes identically when $z=0$, i.e., in the absence of dislocations. Furthermore, configurations with only a single dislocation present cannot contribute to the equilibrium free energy of the commensurate phase since, in the thermodynamic limit, such a configuration must contain p semi-infinite domain walls. Thus in the commensurate phase the singular part of the partition function of a system of area A with, say, periodic boundary conditions, takes the form

$$Z_s\approx e^{Af_s}\approx1+\tfrac{1}{2}AW''_{-}(0)(-\delta)^{2\theta_p+3/2}z^2+O(z^4) . \tag{8.3}$$

The term of order z^2 must arise simply from summing over all configurations in which only two dislocations are present. To obtain the dislocation exponent, θ_p, we may thus examine the restricted partition function, $Z^{(2)}(\delta)$ which represents a sum over all configurations of two dislocations; when $\delta\to0-$ its singular part should vanish as $(-\delta)^{2\theta_p+3/2}$.

A. Dislocation correlations

To study $Z^{(2)}(\delta)$ we must calculate the dislocation correlation function $C_p(x,y;\delta)$, which, as defined, for example, by Schulz, Halperin, and Henley[43] derives from a still further restricted partition function, namely, a sum over those domain-wall configurations in which one dislocation is located at the origin (0,0) while the second one is at the point (x,y). Schulz *et al.*[43] have calculated the asymptotic form of $C_p(x,y;\delta)$ in the weakly incommensurate phase for distances much greater than the correlation lengths $\xi_{\parallel}$ and $\xi_{\perp}$ introduced in Sec. VII. Here we will obtain the scaling form and critical exponents for $C_p(x,y;\delta)$ in the commensurate phase. However, the scaling form for $C_p(x,y;\delta)$ also applies in the incommensurate phase with the results of Schulz *et al.*[43] serving to provide a limiting form for the scaling function.

A typical configuration in the sum for $C_4(x,y;\delta)$ is illustrated in Fig. 9. It consists, in the random-walk picture, of four walkers who start initially at the origin, i.e., in the dislocation core, and then walk upwards for $n=y/b_{\parallel}$ steps, where $b_{\parallel}$ is of the order of the underlying lattice spacing in the y direction.[42,75] The walkers' paths never meet or cross but finally they all reunite at $x=mb_{\perp}$, where $b_{\perp}(T)$, which is given more explicitly in (7.2), represents the root-mean-square transverse displacement of a walker in a single step.[42,75]

If there is only a single walker, the problem posed is standard and for $n=y/b_{\parallel}\gg1$ one has

$$C_1(x,y)\approx e^{-\bar{\Sigma}y}e^{-x^2/2Dy}/(2\pi Dy)^{1/2}\ , \tag{8.4}$$

where $\bar{\Sigma}=\Sigma/k_BT$ is the reduced tension for a wall parallel to the y axis, while the diffusion constant for a walk is given by

$$D(T,\zeta)=b_\perp^2/b_{||}\ , \tag{8.5}$$

which is presumed to be smoothly varying and nonvanishing throughout the transition region. Note that $e^{-\bar{\Sigma}y}$ represents the total weight of all (single) random walks of $n=y/b_{||}$ steps from the origin. The remaining factors in (8.4) represent the fraction of n step walks which terminate at $x=mb_\perp$.

Now recall, from (7.7), (7.16), and (7.17) of the preceding section, how the correlation lengths at the transition to the commensurate phase vary; specifically, we may write

$$\xi_{||}\approx k_BT/\sigma'\,|\,\delta\,|\approx|\,\bar{\Sigma}\,|^{-1},\quad \xi_\perp\approx c_0b_\perp/|\,\delta\,|^{1/2}\ , \tag{8.6}$$

where we have introduced the dimensionless ratio

$$c_0^2=b_{||}\sigma'/k_BT\ . \tag{8.7}$$

Thus, anticipating our general result, we see that the form of $C_1(x,y)$ obeys the scaling law

$$C_p(x,y)\approx|\,\delta\,|^{p^2/2}Q_p^-(x/\xi_\perp,y/\xi_{||})\ , \tag{8.8}$$

for $y\gg b_{||}$; the superscript minus simply serves as a reminder that the commensurate phase, i.e., $\delta\le 0$, is under consideration.

To our knowledge the general case of p walkers reuniting has not been discussed in the literature. As we show in Appendix A, however, it may be handled by diffusion theory methods; the case $p=2$ is analyzed in detail in Ref. 28. The answer is surprisingly simple: We find the scaling function is given by

$$Q_p^-(X,Y)=(c_p/b_\perp)e^{-p(Y+X^2/2Y)}/(2\pi Y)^{p^2/2}\ , \tag{8.9}$$

where c_p is a numerical coefficient.

The results for $C_p(x,y)$ embodied in (8.8) and (8.9) are valid in the commensurate phase for distances x and y large compared with the dislocation core dimensions of order $b_\perp$ and $b_{||}$, respectively. Schulz, Halperin, and Henley, in a similar calculation,[43] have studied the same correlation function inside the *incommensurate* phase for separations large compared with the *correlation lengths* $\xi_\perp$ and $\xi_{||}$ (which, near the transition, are much larger than $b_\perp$ and $b_{||}$). For even integral p and $y=0$ they obtain, in our notation,

$$C_p(x,0;\delta)\approx c_p^\perp(\delta\xi_\perp/x)^{p^2/2}\ , \tag{8.10}$$

where $c_p^\perp$ is a constant. (The Fermi momentum k_F in Schulz *et al.* corresponds to $1/\xi_\perp\sim\delta^{1/2}$.) Notice that this is again consistent with the scaling form (8.8), although the complementary scaling function $Q_p^+(X,Y)$ for $\delta>0$ must now be used: This must match $Q_p^-(X,Y)$ appropriately in the limit $X,Y\to 0$ which corresponds to $\delta\to 0$ at fixed x and y. Note, however, that the scaling function (8.9) has an essential singularity in this limit so that the behavior as $Y\to 0$ is nonuniform. For $p=2$ Schulz *et al.* actually found the exact result which then yields the scaling form

$$Q_2^+(X,0)=c_2^\perp X^{-2}(1-X^{-2}\sin^2X)\ . \tag{8.11}$$

By employing a continuum limit Schulz *et al.* also obtained

$$C_p(x,y;\delta)\sim[(x/\xi_\perp)^2+(y/\xi_{||})^2]^{-p^2/4}\ , \tag{8.12}$$

valid for general $y\gg\xi_{||}$ and $x\gg\xi_\perp$. However, they did not find the behavior of the prefactor as $\delta\to 0$. We may anticipate from scaling that this should vary as $|\,\delta\,|^{p^2/2}$ and thence that the incommensurate dislocation-dislocation correlation scaling function behaves asymptotically as

$$Q_p^+(X,Y)\sim(X^2+Y^2)^{-p^2/4} \tag{8.13}$$

when $X,Y\to\infty$. The result (8.12) confirmed a previous, indirect analysis of the dislocation interactions based on the elastic constants of the incommensurate phase in the absence of dislocations.[5,19] Recall now that the incommensurate phase exhibits algebraic decay of correlations and hence is a *critical phase.* One can thus appeal to the Kadanoff-Wegner criterion for the relevance of a perturbation: Specifically,[50] an operator $A(\vec{r})$ represents a relevant perturbation of a critical point if its correlation function $\langle A(\vec{r})A(\vec{r}')\rangle_c$, evaluated *at* criticality, decays as $1/|\,\vec{r}'-\vec{r}\,|^{2\omega_A}$ with $\omega_A<d$. This follows[50] because the associated renormalization-group eigenvalue $\lambda_A=d-\omega_A$ and crossover exponent, $\phi_A(=\lambda_A/\lambda_{\mathscr{E}}$, where $\lambda_{\mathscr{E}}$ is the thermal eigenvalue) are then positive. One thus concludes that a weakly incommensurate uniaxial surface phase is unstable to dislocations if $\frac{1}{2}p^2<2d=4$, i.e., if $p<\sqrt{8}$. This agrees, as it must, with the analysis[5,19] based on the Kosterlitz-Thouless and Halperin-Nelson-Young criteria.[5,19]

B. Singularities in the commensurate phase

Now, by the arguments following (8.3), the behavior of the two-dislocation partition function, $Z^{(2)}$, as the thermodynamic limit is approached is given by

$$Z^{(2)}/A\approx\int_{b_{||}}^{\infty}b_{||}^{-1}dy\int dx\,C_p(x,y;\delta)\ , \tag{8.14}$$

and has a leading singular part varying as $|\,\delta\,|^{2\theta_p+3/2}$. The lower cutoff on the y integral recognizes the finite size of a dislocation core. On using the scaling form (8.8) and (8.9) one hence finds that the singular part varies as

$$f_s(\delta)\propto Z_s^{(2)}(\delta)\sim|\,\delta\,|^{(p^2-3)/2}\ \text{ or }\ |\,\delta\,|^{(p^2-3)/2}\ln|\,\delta\,|^{-1}\ , \tag{8.15}$$

where the second form applies only when $p^2>1$ is an odd integer. We thus conclude that the dislocation crossover exponent is determined by

$$\theta_p=\tfrac{1}{4}(p^2-6)\ . \tag{8.16}$$

It follows from this that dislocations are *relevant* at the two-dimensional uniaxial commensurate-incommensurate transition when $p^2<6$. This is consistent with Bohr's[44] calculations for $p=2$ where dislocations were found to induce crossover to a phase transition in the Ising universal-

ity class. Our result gives a crossover exponent $-\theta_2=\frac{1}{2}$ and the singular part of Bohr's expression for the free energy does indeed asymptotically fit the scaling form (8.1) with scaling functions (for suitably normalized δ and z)

$$W_{\pm}(u)=\int_0^{\infty} dq\{q^2\mp 1+\tfrac{1}{2}u^2-[(q^2\mp 1)^2+q^2u^2]^{1/2}\}/2\pi \ . \tag{8.17}$$

These scaling functions display the Ising-like logarithmic singularities expected for $\delta\to 0$ with $z>0$, namely,

$$W_{\pm}(u)=\frac{u^3}{2\pi}\left[\frac{1}{3}\mp\frac{1}{u^2}-\frac{2}{u^4}\ln u+O\left[\frac{1}{u^4}\right]\right] \tag{8.18}$$

for $u=z/|\delta|^{1/2}\to\infty$. Note that when this is substituted in (8.1) the free energy has analytic terms in δ (for δ small) plus a $\delta^2\ln|\delta|$ singularity. The incommensurate phase present for $z=0$ and $\delta>0$ also melts in an Ising-like transition as the dislocation fugacity z is increased from zero; the scaling function for small u behaves as

$$W_{+}(u)=\frac{1}{2\pi}[-\tfrac{4}{3}+\tfrac{1}{2}u^2\ln u+O(u^2)] \ . \tag{8.19}$$

In the commensurate phase ($\delta<0$) the scaling function in the limit of small dislocation fugacity behaves as $W_{-}(u)\sim u^2=z^2/|\delta|$, reflecting the fact that all possible fluctuations involve at least two dislocations.

For this $p=2$ system Bohr[44] also finds that the correlation function in the x direction,

$$G(x)=\langle(-1)^{n(0)-n(x)}\rangle-\langle(-1)^{n(0)}\rangle\langle(-1)^{n(x)}\rangle \ , \tag{8.20}$$

decays asymptotically as

$$G(x)\sim \mathrm{Re}(e^{ik^*x}) \ , \tag{8.21}$$

as long as $\delta\neq 0$ and $z\neq 0$, where k^* is the nearest zero above the real axis in the "single-particle" spectrum of the transfer matrix

$$E(k)\approx[(\delta-k^2)^2+z^2k^2]^{1/2} \ . \tag{8.22}$$

A correlation length and incommensurability may thereby be defined via

$$k^*=\bar{q}+i/\xi_x \ , \tag{8.23}$$

and both will scale in the same fashion as the free energy, namely,

$$\xi_x\approx|\delta|^{-1/2}X_{\pm}(z/|\delta|^{1/2}) \ , \tag{8.24}$$

$$\bar{q}\approx|\delta|^{1/2}Q_{\pm}(z|\delta|^{1/2}) \ . \tag{8.25}$$

The scaling functions are easily found to be

$$X_{-}(u)=(1+\tfrac{1}{4}u^2)^{1/2}+\tfrac{1}{2}u, \quad Q_{-}(u)=0 \ , \tag{8.26}$$

$$X_{+}(u)=\tfrac{1}{2}u+(\tfrac{1}{4}u^2-1)^{1/2}, \quad Q_{+}(u)=0 \ \text{ for } u\geq 2 \ , \tag{8.27}$$

$$X_{+}(u)=2/u, \quad Q_{+}(u)=(1-\tfrac{1}{4}u^2)^{1/2} \ \text{ for } u\leq 2 \ .$$

In contrast to this soluble $p=2$ case, for $p^2>6$ and, in particular, for $p\geq 3$, dislocations prove to be *irrelevant* so that, for sufficiently small but finite dislocation fugacity or density, the transition remains in the same universality class as in the absence of dislocations. However, the dislocations still mediate divergent fluctuations in the commensurate phase, somewhat reminiscent of droplet fluctuations at a first-order transition,[81] and thus induce critical singularities on the commensurate side of the phase transition. These new singularities represent corrections to scaling that are absent unless dislocations occur and, therefore, are weaker by a correction to scaling exponent equal to $2\theta_p$ than the corresponding singularities on the the incommensurate side of the transition. Thus the specific-heat singularity which, by (7.13), is given by $\alpha=\frac{1}{2}$ on the incommensurate side, follows by this rule or directly from (8.15) as

$$\alpha_p'=\tfrac{1}{2}(7-p^2), \quad p>\sqrt{6} \ . \tag{8.28}$$

This describes a cusped, $|\delta|\ln|\delta|^{-1}$ singularity for $p=3$. Likewise, the susceptibility $\chi=\partial^2 f/\partial h^2$ considered in (7.14) diverges with an exponent $\gamma=\frac{3}{2}$ in the incommensurate phase but displays only a weaker singularity with exponent

$$\gamma_p'=\tfrac{1}{2}(9-p^2) \ , \tag{8.29}$$

in the commensurate phase. For $p=3$ this corresponds to a divergence of χ as $\ln|\delta|^{-1}$ but represents no divergence in χ, or even in $\partial\chi/\partial\delta$, for $p\geq 4$. Despite their weakness these commensurate phase singularities might be observable in sufficiently precise careful measurements.

C. Phase diagrams

It is interesting to consider the evolution of the (δ,z) phase diagram of this system of fluctuating domain walls with dislocations as p varies. Our expectations are embodied in Fig. 11. In the absence of dislocations, i.e., for fugacity $z=0$, the phase diagram is independent of p, consisting of a critical point, marked F, separating the *inert* or *frozen* commensurate phase with no critical fluctuations at all from the incommensurate phase. The phase transition at F is in the free-fermion universality class since the transfer matrix may be modeled as a noninteracting one-dimensional Fermi gas,[43] which has a phase transition when the chemical potential of the fermions passes through the band edge. In this fermion representation the spatial y axis is again to be thought of as a time direction and the domain walls correspond to the world lines of the fermions. Allowing dislocations of fugacity z corresponds to adding terms in the fermion Hamiltonian which create and annihilate p fermions near one another with coupling constant z.[43,44]

For $p^2<6$ the dislocations are relevant at F, which is therefore a multicritical point. The incommensurate phase present for zero dislocation fugacity is unstable to dislocations for $p^2<8$ and so, as is illustrated in Fig. 11, it melts immediately into a disordered phase as the dislocation fugacity increases from zero.[5,19] Note that the relevance of the dislocations at the commensurate-incommensurate critical point, F, and *inside* the "critical" incommensurate phase are two distinct issues. When, for

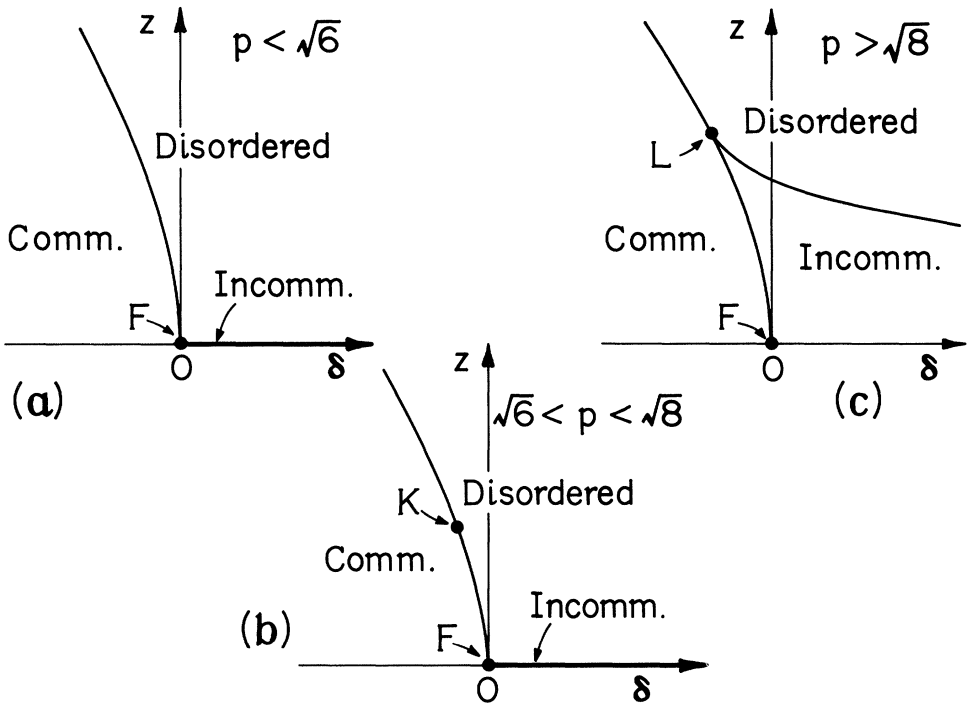

FIG. 11. Phase diagrams for the two-dimensional domain-wall wandering model with dislocations allowed. When $z=0$ the field δ is proportional to the individual domain-wall tensions which are positive for $\delta<0$ but change sign at $\delta=0$ allowing an incommensurate phase to appear for $\delta>0$. The activity or fugacity, z, controls the density of dislocations. The free-fermion critical point, F, is unstable to dislocations for $p<\sqrt{6}$. A new multicritical point, K, splits off at $p=\sqrt{6}$ and becomes a Lifshitz point, L, at $p=\sqrt{8}$.

$p^2<6$, the dislocations are relevant at F, the commensurate-disordered phase boundary at nonzero dislocation fugacity is in a different universality class than F; for $p=2$ this is just the standard Ising universality class.[44] At $p^2=6$ the dislocations become *marginal* at F and a preliminary analysis indicates that they are, in fact, *marginally relevant.* Thus as p increases beyond $\sqrt{6}$ a new multicritical point, say K, emerges from F; this new multicritical point becomes a Lifshitz point, L, for $p^2>8$ when the incommensurate phase becomes stable to dislocations. The phase boundary between L and F is in the same free-fermion universality class as is F, however, as discussed above, corrections to scaling give critical singularities in the commensurate phase that are not present at F. The commensurate-disordered phase boundary beyond L is presumably in the p-state chiral universality class introduced in Sec. IV. The scenario presented in Fig. 11 is certainly consistent with other treatments, namely, the analytic results[44] for $p=2$ and Monte Carlo[25] and series-expansion[27] results for $p=3$. What happens to the Lifshitz point beyond $p=3$ is a matter of speculation and certainly depends on further details of the system. In a chiral *Potts* model (as against *clock* model) examined by Kardar[26] the Lifshitz point persists even for $p>4$ where the commensurate-disordered phase transition becomes first order. However, as is discussed in Section V the Lifshitz point in the chiral clock-model phase diagram must disappear when p exceeds 4 since the incommensurate phase then completely separates the commensurate and disordered phases as shown in Fig. 5(d).

IX. DISLOCATIONS AND THE CHIRAL CLOCK MODELS

The dislocations discussed in the previous few sections and illustrated in Figs. 9 and 10 are topologically stable: As explained in Sec. VII the existence of a dislocation may be discerned from the behavior of the order parameter on a closed contour surrounding it.[77] If successive domains are identified by the spin state, $n=0,1,\ldots,p-1$, that the clock model spins within the domains preferentially occupy, then upon crossing each elementary domain wall, n changes by $\delta n=\pm 1 \pmod p$. The line integral of δn along a closed contour oriented, say, clockwise and enclosing a single dislocation, will take the two possible values,

$$\oint dn=\pm p\ , \tag{9.1}$$

but will vanish if no dislocation is enclosed.

Such a topological definition of a dislocation may be extended in the context of the chiral clock models (2.1) to ascribe definite *microscopic* locations to dislocations in any configuration of spins in the model. Thus on a square lattice each elementary square may be assigned a dislocation state by performing a sum analogous to (9.1) over its four perimeter bonds. The change in n upon traversing the bond from a site i to its nearest neighbor j is defined conveniently for the present purpose as

$$(\delta n)_{ij}=n_j-n_i \pmod p \quad \text{with} \quad |(\delta n)_{ij}| \le \tfrac{1}{2}p\ . \tag{9.2}$$

For odd p this determines each $(\delta n)_{ij}$ uniquely but for even p a further convention is needed to fix $(\delta n)_{ij}$ in cases where $|(\delta n)_{ij}| = \frac{1}{2}p$; the convention adopted is not crucial provided it respects the antisymmetry relation

$$(\delta n)_{ij} = -(\delta n)_{ji} \ . \tag{9.3}$$

Then the number of dislocations or "vortices" v_{ijkl} contained in the square comprised, in, say, clockwise order, of sites i, j, k, and l is

$$v_{ijkl} = |(\delta n)_{ij} + (\delta n)_{jk} + (\delta n)_{kl} + (\delta n)_{li}|/p \ . \tag{9.4}$$

The dislocation density may thus be expressed as a local operator that couples the spins around each elementary square (or "plaquette") of the lattice.

In order to study the effects of varying the dislocation fugacity, z, on the behavior of the chiral clock model one may simply introduce the dislocation core energy, $E_0 = -k_B T \ln z$, as a parameter by extending the Hamiltonian to

$$\mathscr{H} = \mathscr{H}_0 + E_0 \sum_{(ijkl)} v_{ijkl} \ , \tag{9.5}$$

where $\mathscr{H}_0$ is the original chiral Hamiltonian (2.1) and the sum runs over all the elementary squares of the lattice. In the limit of no dislocations ($E_0 \to \infty$) the phase diagrams of this model for various p should resemble those obtained recently from an exact solution of the one-dimensional quantum sine-Gordon model by Haldene, Bak, and Bohr.[15] For $p \geq 5$ there are no *free* dislocations in the vicinity of the commensurate phase since the disordered fluid, which is characterized by a density of free dislocations is completely separated by the incommensurate phase. Thus increasing the dislocation core energy, E_0, from zero should not produce any qualitative changes in the phase diagram shown in Fig. 5(d). As the core energy is sufficiently *decreased,* however, the nature of the phase diagrams must eventually change from those shown in Fig. 5 for *all* p because for $E_0 \ll -J$ the ground state will no longer be ferromagnetically ordered, but will rather become some sort of "vortex glass" that contains the maximum possible density of dislocations: Compare with the discussion of Swendson[82] who considers a related two-dimensional model based on continuous XY spins.

Let us consider, in particular, the case $p = 3$. The sine-Gordon analysis of Haldane, Bak, and Bohr should yield the correct phase diagram for the chiral clock model in the *limit* of zero dislocation fugacity, i.e., $E_0 \to +\infty$. Their results are embodied in the (T, Δ, z) phase diagram presented in Fig. 12. In the absence of dislocations, i.e., *in* the $z = 0$ plane, only two phases occur, namely a low-temperature commensurate phase and a high-temperature incommensurate phase, separated by the critical line QC_0 in Fig. 12. The point Q on the $\Delta = 0$ axis has a multicritical character as will shortly become even more evident. As we have discussed above, the commensurate-incommensurate transition for $p = 3 > \sqrt{6}$ is stable under the introduction of dislocations. Thus as z increases from zero the critical line QC_0 develops into a critical surface, namely, QC_0CL in Fig. 12, separating commensurate and incommensurate regions. However, the $z = 0$ *in*commensurate *phase* becomes *un*stable to dislocations above a locus, QI_0, of the form shown by the dotted curve in Fig. 12, as was shown by Haldane *et al.*[15] Thus the locus QI_0 develops, for small z, into a critical surface, QI_0IL, which separates the incommensurate phase from a disordered fluid phase which exists everywhere at high temperatures *except when* $z = 0$.

Now the dislocations are also relevant at the symmetric ($\Delta = 0$) multicritical point Q.[49,15] In addition, however, the numerical evidence[25,27] suggests the presence of a distinct Lifshitz point at $\Delta > 0$ when dislocations are allowed. The simplest phase diagram consistent with these various conclusions has the form shown in Fig. 12. It contains a line of three-state Potts critical points, QP and a line of Lifshitz points, QL. These lines both emerge from the multicritical point Q and they bound a critical surface, QPL, in the $p = 3$ chiral melting universality class. Note that the incommensurate phase at $z = 0$ is stable to dislocations in the region bounded by the lines QI_0 and QC_0, a region that extends all the way to the symmetric multicritical point Q. Thus even if a line of Lifshitz points (QL in Fig. 12) also goes to Q, as we suggest it may, this will not be revealed by calculations carried only to leading order in

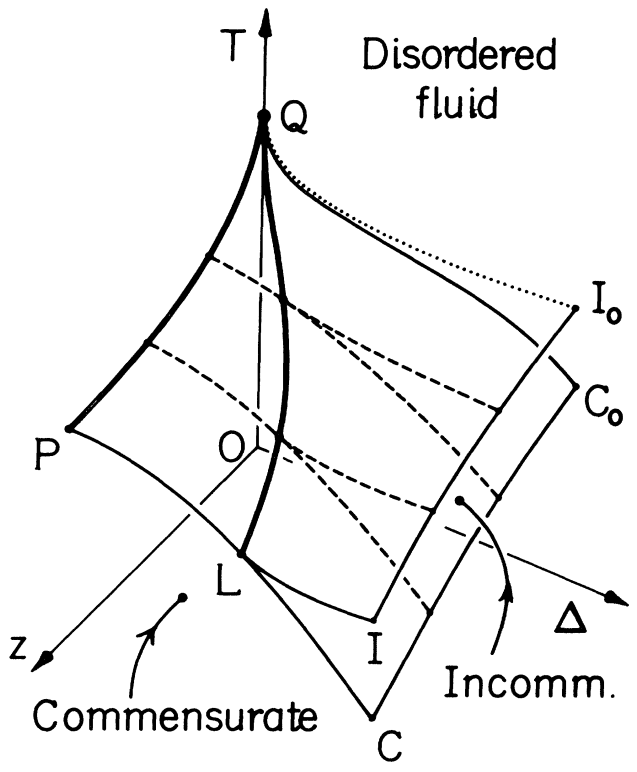

FIG. 12. Anticipated phase diagram of the two-dimensional three-state extended chiral clock model, (9.5), as a function of dislocation fugacity, z. Broken curves represent the phase boundaries at fixed values of z. The disordered fluid phase fills the region above the surface $QPLII_0$, except for the $z = 0$ plane, where the incommensurate phase persists above the line QI_0. The commensurate phase lies below the surface $QPLCC_0$. The lines QP and QL represent Potts and Lifshitz multicritical points, respectively, and bound a critical surface in the new chiral melting universality class.

the dislocation fugacity such as reported by Haldane *et al.*[15] and by Schulz[16] who argue that the Lifshitz line is not present for small dislocation activity, z.

A similar phase diagram to Fig. 12 might apply for $p=4$ but then the line QP of symmetric ($\Delta=0$) multicritical points is expected[49] to have exponents varying continuously with z. This suggests that the Lifshitz line for $p=4$, if it exists at all, might, in contrast to Fig. 12, possibly terminate at a point on the line QP of symmetric multicriticality at which z is nonzero. Thus Lifshitz points might exist for $p=4$ only at sufficiently large dislocation fugacity. Further analytical work is clearly necessary to check this speculation and to test our expectations for $p=3$.

ACKNOWLEDGMENTS

We are indebted to Daniel S. Fisher, Bertrand I. Halperin, and Heinz J. Schulz for informative discussions and comments. The collaboration of Anthony M. Szpilka on a study (Ref. 28) of the chiral clock model in two dimensions has been appreciated. The support of the National Science Foundation through a grant from the Condensed Matter Theory Program and, in part, through the Materials Science Research Center at Cornell University, is gratefully acknowledged.

APPENDIX A: THE REUNIONS OF p WALKERS

In this appendix we discuss the problem of p identical walkers, initially close together, that walk on a line without passing one another and we ask for the probability of a "reunion" after a long time. More concretely, let $x_j \equiv x_j(t)$, with $j=1,2,\ldots,p$, denote the coordinate of the jth walker at time t and let $x_{j,0} \equiv x_j(0)$ denote the corresponding initial coordinates which we suppose satisfy

$$-a < x_{1,0} < x_{2,0} < \cdots < x_{p,0} < a \ , \tag{A1}$$

where a is a fixed bound. (In our current application to domain-wall systems x_j represents the x coordinate of the jth domain wall at a level $y \propto t$, while a measures the size of a dislocation core.) We desire the probability distribution, $W_p(\vec{x}_0 \Longrightarrow \vec{x};t)$, that the walkers proceed *without passing,* i.e., maintaining the inequalities

$$x_{j-1}(t') < x_j(t'), \quad j=2,3,\ldots,p \quad \text{for } t' \le t \ , \tag{A2}$$

from their initial positions specified by $\vec{x}_0=(x_{1,0},\ldots,x_{p,0})$ to final positions given by $\vec{x}=(x_1,\ldots,x_p)$ at time t.

Perhaps the most natural setting for the problem is on a lattice with discrete time where, on every tick of the clock, each walker takes a nearest-neighbor step to right or left with equal probabilities and the walkers start only on even numbered lattice sites.[28] However, since we are here interested only in long times, we shall consider, from the outset, the simpler case of the continuum limit (i.e., Brownian motion) in which the probability distribution for *p free, unrestricted,* or independent walkers is simply

$$W_p^0(\vec{x}_0 \Longrightarrow \vec{x},t) = e^{-|\vec{x}-\vec{x}_0|^2/2Dt}/(2\pi Dt)^{p/2} \ . \tag{A3}$$

Here the diffusion constant D sets the scale since the mean-square displacement of a single walker is just $\langle (x_j - x_{j,0})^2 \rangle = Dt$.

Now if we regard (A3) as describing the motion of a single, *compound walker* who moves in a p-dimensional space with position coordinate $\vec{x}$, the restrictions (A2) mean that the compound walker must not cross any of the linear manifolds $x_1=x_2$, $x_2=x_3$, ..., or $x_{p-1}=x_p$. This restriction may be viewed as posing an *absorbing boundary* condition requiring that $W_p(\vec{x}_0 \Longrightarrow \vec{x},t)$ vanish identically on all these manifolds. Because the manifolds are linear the corresponding diffusion problem can be solved by the method of images: Specifically, unrestricted walkers of positive and negative weights are started at $\vec{x}_0$ and its mirror images and proceed to walk according to (A3). Provided the initial weights are chosen so that the total distribution is antisymmetric under reflection in each manifold $x_{j-1}=x_j$, the subsequent distribution will vanish on each manifold for all times and, hence, solves the problem.

To obtain an analytic expression let g denote an element of the permutation group on p objects, S_p, which permutes the components $v_j \equiv (\vec{v})_j$ of a p-vector $\vec{v}$. Then, to generate W_p, we must start a walker with weight $\epsilon(g)$ at each mirror-image point $g\vec{x}_0$, where $\epsilon(g)=+1$ for even permutations (i.e., for an even number of reflections) and $\epsilon(g)=-1$ for odd permutations (and hence for an odd number of reflections). For $\vec{x}$ satisfying (A2) this yields

$$W_p(\vec{x}_0 \Longrightarrow \vec{x},t) = \sum_{g \in S_p} \epsilon(g) W_p^0(g\vec{x}_0 \Longrightarrow \vec{x},t) \ . \tag{A4}$$

Under the permutations we have $|g\vec{x}_0|^2 = |\vec{x}_0|^2$ and so the result can be written

$$W_p(\vec{x}_0 \Longrightarrow \vec{x},t) = U_p(\vec{x}_0,\vec{x};t) \frac{e^{-(|\vec{x}|^2+|\vec{x}_0|^2)/2Dt}}{(2\pi Dt)^{p/2}} \ , \tag{A5}$$

where the antisymmetrized sum is defined by

$$U_p(\vec{v}_0,\vec{v},t) = \sum_{g \in S_p} \epsilon(g) \exp(\vec{v}\cdot g\vec{v}_0/Dt) \ . \tag{A6}$$

Now we wish to focus attention on the asymptotic probability, for long times, of a *reunion* at $\bar{x}$, which we define by the condition

$$\bar{x}-a < x_1 < x_2 < \cdots < x_p < \bar{x}+a \ , \tag{A7}$$

at time t where, with no loss of generality we also suppose that

$$\sum_{j=1}^{p} x_{j,0} = \sum_{j=1}^{p} (x_j - \bar{x}) = 0 \ , \tag{A8}$$

so that the origin is placed at the mean starting position and $\bar{x}$ denotes the mean final position. From this we have

$$\vec{x}\cdot g\vec{x}_0 = \sum_{j=1}^{p} (x_j - \bar{x})(g\vec{x}_0)_j = O(a^2) \ . \tag{A9}$$

To evaluate the factor $U_p(\vec{v}_0,\vec{v};t)$, notice, first, that $\vec{v}\cdot g\vec{v}_0 = g^{-1}(\vec{v}\cdot g\vec{v}_0) = \vec{v}_0 \cdot g^{-1}\vec{v}$ so that U_p is symmetric under the interchange $\vec{v}_0 \Longleftrightarrow \vec{v}$. Second, note that the argument of the exponential may, by (A9), be considered of order a^2/Dt so that an expansion in powers of $\vec{v}_0$ is justi-

fied. The nth term in the expansion is evidently a homogeneous polynomial of degree n in the p variables v_j. However, only totally antisymmetric polynomials can survive the sum over g. The lowest order such polynomial is of degree

$$n=n_p\equiv\tfrac{1}{2}p(p-1)\ , \tag{A10}$$

and may be represented by a Vandermonde determinant of order p, with elements $V_{ij}=v_j^{i-1}$, namely,

$$V_p(\vec{v})=|\,V_{ij}\,|=|\,v_j^{i-1}\,|_p=\prod_{j>k}^{p}(v_j-v_k)\ . \tag{A11}$$

Hence we may write

$$U_p(\vec{x}_0,\vec{x};t)\approx u_p V_p(\vec{x}_0)V_p(\vec{x})/(Dt)^{n_p}\ , \tag{A12}$$

with corrections of relative order (a^2/Dt), while the coefficient u_p is determined by the identity

$$u_p V_p(\vec{v}_0)V_p(\vec{v})\equiv\frac{1}{n_p!}\sum_{g\in S_p}\epsilon(g)(\vec{v}\cdot g\vec{v}_0)^{n_p}\ . \tag{A13}$$

To use this consider the differential operator

$$\mathscr{D}_p=\frac{d^0}{dv_1^0}\frac{d}{dv_2}\frac{d^2}{dv_3^2}\cdots\frac{d^{p-1}}{dv_p^{p-1}}\ , \tag{A14}$$

which is of order n_p. One finds, recursively,

$$\mathscr{D}_p V_p(\vec{v})=\mathscr{D}_{p-1}\frac{d^{p-1}\,|\,v_j^{i-1}\,|_p}{dv_p^{p-1}}$$

$$=(p-1)!\mathscr{D}_{p-1}V_{p-1}(\vec{v})=\prod_{r=1}^{p-1}r!\ , \tag{A15}$$

and, for the right-hand side of (A13),

$$\mathscr{D}_p(\vec{v}\cdot g\vec{v}_0)^{n_p}=\frac{n_p!}{(n_p-p+1)!}(g\vec{v}_0)_p^{p-1}\mathscr{D}_{p-1}(\vec{v}\cdot g\vec{v}_0)^{n_p-p+1}=n_p!\prod_{j=1}^{p}(g\vec{v}_0)_j^{j-1}=n_p!v^0_{g_1,0}v^1_{g_2,0}\cdots v^{p-1}_{g_p,0}\ , \tag{A16}$$

where $(g_1,g_2,\ldots,g_p)=g(1,2,\ldots,p)$. Upon performing the sum over g this last expression yields $n_p!V(\vec{v}_0)$. Substitution in (A13) thus gives

$$u_p=\frac{1}{1!2!\cdots(p-1)!}\ . \tag{A17}$$

The desired result for the asymptotic probability of reunion now follows from (A5) and (A12) as

$$W_p(\vec{x}_0\Longrightarrow\vec{x},t)=\frac{e^{-p\bar{x}^2/2Dt}}{(2\pi)^{p/2}(Dt)^{p^2/2}}\prod_{j>k\geq 1}^{p}(x_{j,0}-x_{k,0})(x_j-x_k)\frac{1+O(a^2/Dt)}{1!2!\cdots(p-1)!}\ , \tag{A18}$$

where the convention (A8) is to be recalled. If the initial and final positions of the walkers are equally spaced with

$$x_{j+1,0}-x_{j,0}=x_{j+1}-x_j=a_0\ , \tag{A19}$$

the products simplify and one obtains

$$W_p(\bar{x},t)\approx a_0^{p(p-1)}\left[\prod_{r=1}^{p-1}r!\right]e^{-p\bar{x}^2/2Dt}/(2\pi)^{p/2}(Dt)^{p^2/2}\ . \tag{A20}$$

If one now integrates (or, for a lattice, sums) over the position $x=\bar{x}$, of the reunion, one finds that the total probability (or "number" of walks of $n\propto t$ steps) varies as

$$g^{(p)}(t)\approx g_0^{(p)}/t^{(p^2-1)/2}\ , \tag{A21}$$

as stated in (6.28). The singular behavior of the corresponding generating function, $\mathscr{G}_p(w,x)$, defined in (6.13) is then easily seen to be as reported in (6.18) and (6.19).

APPENDIX B: ONE-DIMENSIONAL CHIRAL CLOCK MODEL

In this appendix we examine the critical and multicritical behavior of the p-state chiral clock model (2.1) on a one-dimensional, linear chain. Since this is a one-dimensional system with short-range interactions the correlation length remains finite for all nonzero temperatures. Nevertheless, the p-state chiral clock models for $p>2$ each exhibit a chiral ordering transition governed by a universal chiral scaling function for the correlations, just as postulated generally in (4.6), as well as a symmetric ($\Delta=0$) multicritical point near which the free energy is governed by a multicritical scaling function of the form (3.2).

The $p\times p$ transfer matrix, $\underline{V}$, for the one-dimensional p-state clock model has elements

$$V_{kl}=\exp\{K\cos[2\pi(l-k+\Delta)/p]\}\ , \tag{B1}$$

where $K=J/k_BT$. These specify a cyclic matrix which has eigenvalues

$$\lambda_m=\sum_{k=0}^{p-1}V_{0k}e^{2\pi imk/p}\ , \tag{B2}$$

where $m=0,1,\ldots,p-1$.[23] The free energy per spin, f, is obtained as usual from the largest eigenvalue, λ_0, via

$$f(T,\Delta)=-k_BT\ln\lambda_0$$

$$=-J\cos(2\pi\Delta/p)$$

$$-k_BT\sum_{k=1}^{p-1}[V_{0k}/V_{00}+O(V_{0k}^2/V_{00}^2)]\ , \tag{B3}$$

where the second line exhibits the low-temperature behavior near the ferromagnetic ordering transition that occurs at $T=0$ for $|\Delta|<\frac{1}{2}$. In the low-temperature limit the terms from $k=1$ and $p-1$ dominate the sum. Inserting (B1) reveals that the singular part of the free energy behaves, for $T\to 0$ and $|\Delta|<\frac{1}{2}$, as

$$f_s \equiv f + J\cos(2\pi\Delta/p) \approx -k_B T \exp\left[-K\left[1-\cos\frac{2\pi}{p}\right]\cos\frac{2\pi\Delta}{p}\right] \times \cosh\left[K\sin\frac{2\pi}{p}\sin\frac{2\pi\Delta}{p}\right] . \quad \text{(B4)}$$

In the vicinity of the symmetric multicritical point, $\Delta=0$, $T_c^0=0$, this reduces to a scaling form like (3.2), as expected for general dimensionalities, namely,

$$f_s \approx -k_B T \exp\left[-K\left[1-\cos\frac{2\pi}{p}\right]\right] W_p\left[\frac{J\Delta}{k_B T}\right] , \quad \text{(B5)}$$

where the scaling function is

$$W_p(x)=\cosh[\sin(2\pi/p)(2\pi x/p)] . \quad \text{(B6)}$$

The basic spin-spin correlation function for this one-dimensional model is[23]

$$G(n)\equiv\langle\exp[2\pi i(s_n-s_0)/p]\rangle=(\lambda_1/\lambda_0)^n , \quad \text{(B7)}$$

for $n\geq 0$, while for $n\leq 0$ we have

$$G(n)=G^*(-n)=(\lambda_1^*/\lambda_0)^{|n|} . \quad \text{(B8)}$$

Fourier transformation yields the structure factor

$$S(q)=\sum_n e^{iqn}G(n) =(1-e^{-2\kappa})/[1-2e^{-\kappa}\cos(q-\bar{q})+e^{-2\kappa}] , \quad \text{(B9)}$$

where the inverse correlation length κ and the incommensurability $\bar{q}$ are defined, in the usual way, via

$$\lambda_1/\lambda_0=\exp(-\kappa+i\bar{q}) . \quad \text{(B10)}$$

Here and above the lattice spacing has been taken as $a=1$. In the limit $T\to 0$ we find, for all chiral fields in the range $0<\Delta<\frac{1}{2}$,

$$\kappa-i\bar{q}\approx(\lambda_0-\lambda_1)/\lambda_0\approx(1-e^{2\pi i/p})V_{01}/V_{00} , \quad \text{(B11)}$$

so that the correlation length is given by

$$\kappa\approx 2\sin^2(\pi/p)V_{01}/V_{00} , \quad \text{(B12)}$$

while the incommensurability satisfies

$$\bar{q}\approx w_0\kappa \text{ with } w_0=\cot(\pi/p) . \quad \text{(B13)}$$

Thus in the scaling limit $qa\ll 1$, $T\to 0$, the structure factor scales as in (4.6), namely as

$$S(q)\approx 2\kappa^{-(2-\eta)}D(q/\kappa) , \quad \text{(B14)}$$

where $\eta=1$ and the universal scaling function is simply

$$D(w)=1/[1+(w-w_0)^2] , \quad \text{(B15)}$$

This represents a standard Lorentzian form but with the maximum displaced from the origin as we have argued is to be expected quite generally for a chiral ordering transition. The one-dimensional model therefore confirms all the expected features.

---

*Present address.

[1]P. M. Horn, R. J. Birgeneau, P. Heiney, and E. M. Hammonds, Phys. Rev. Lett. 41, 961 (1978).

[2]A. N. Berker, S. Ostlund, and F. A. Putnam, Phys. Rev. B 17, 3650 (1978).

[3]D. M. Butler, J. A. Litzinger, and G. A. Stewart, Phys. Rev. Lett. 44, 466 (1980).

[4]D. E. Moncton, P. W. Stephens, R. J. Birgeneau, P. M. Horn, and G. S. Brown, Phys. Rev. Lett. 46, 1533 (1981); 49, 1679 (1982).

[5]S. N. Coppersmith, D. S. Fisher, B. I. Halperin, P. A. Lee, and W. F. Brinkman, Phys. Rev. Lett. 46, 549, 869(E) (1981); Phys. Rev. B 25, 349 (1982).

[6]M. Kardar and A. N. Berker, Phys. Rev. Lett. 48, 1552 (1982).

[7]M. Bretz, Phys. Rev. Lett. 38, 501 (1977).

[8]L. D. Roelofs, A. R. Kortan, T. L. Einstein, and R. L. Park, Phys. Rev. Lett. 46, 1465; 47, 1348 (1981); M. Schick, *ibid.* 47, 1347 (1981).

[9]M. Jaubert, A. Glachant, M. Bienfait, and G. Boato, Phys. Rev. Lett. 46, 1679 (1981).

[10]R. D. Diehl and S. C. Fain, Surf. Sci. 125, 116 (1983).

[11]J. P. Jamet, P. Lederer, and A. H. Moudden, Phys. Rev. Lett. 48, 442 (1982).

[12]A. Erbil, A. R. Kortan, R. J. Birgeneau, and M. S. Dresselhaus, Phys. Rev. Lett. 49, 1427 (1982).

[13]S. Aubry in *Solitons and Condensed Matter Physics,* edited by A. R. Bishop and T. Schneider (Springer, New York, 1979); V. L. Pokrovsky, J. Phys. (Paris) 42, 761 (1981).

[14]V. L. Pokrovsky and A. L. Talapov, Phys. Rev. Lett. 42, 65 (1979); Zh. Eksp. Teor. Fiz. 78, 269 (1980) [Sov. Phys.—JETP 51, 134 (1980)].

[15]F. D. M. Haldane, P. Bak, and T. Bohr, Phys. Rev. B 28, 2743 (1983).

[16]H. J. Schulz, Phys. Rev. B 28, 2746 (1983).

[17]P. Bak and J. von Boehm, Phys. Rev. B 21, 5297 (1980).

[18]M. E. Fisher and W. Selke, Phys. Rev. Lett. 44, 1502, 45, E148, (1980); Philos. Trans. R. Soc. London Ser. A 302, 1 (1981).

[19]J. Villain and P. Bak, J. Phys. (Paris) 42, 657 (1981).

[20]W. Selke, Z. Phys. B 43, 335 (1981).

[21]M. E. Fisher and D. A. Huse, in *Melting, Localization and Chaos,* edited by R. K. Kalia and P. Vashishta (Elsevier, New York, 1982).

[22]S. Ostlund, Phys. Rev. B 24, 398 (1981).

[23]D. A. Huse, Phys. Rev. B 24, 5180 (1981).

[24]J. M. Yeomans and M. E. Fisher, J. Phys. C 14, L835 (1981).

[25]W. Selke and J. M. Yeomans, Z. Phys. B 46, 311 (1982).

[26]M. Kardar, Phys. Rev. B 26, 2693 (1982).

[27]S. F. Howes, Phys. Rev. B 27, 1762 (1983).

[28]D. A. Huse, A. M. Szpilka, and M. E. Fisher, Physica 121A,

363 (1983).
[29]R. J. Baxter, J. Phys. A 13, L61 (1980).
[30]W. Kinzel and M. Schick, Phys. Rev. B 24, 324 (1981).
[31]D. A. Huse, Phys. Rev. Lett. 49, 1121 (1982); J. Phys. A (in press).
[32]W. Kinzel, W. Selke, and K. Binder, Surf. Sci. 121, 13 (1982); W. Selke, K. Binder, and W. Kinzel, Surf. Sci. 125, 74 (1983).
[33]E. Domany, M. Schick, J. S. Walker, and R. B. Griffiths, Phys. Rev. B 18, 2209 (1978).
[34]S. Alexander, Phys. Lett. 54A, 353 (1975).
[35]B. Nienhuis, J. Phys. A 15, 199 (1982).
[36]F. Y. Wu, Rev. Mod. Phys. 54, 235 (1982).
[37]D. A. Huse and M. E. Fisher, Phys. Rev. Lett. 49, 793 (1982).
[38]A. Aharony and P. Bak, Phys. Rev. B 23, 4770 (1981).
[39]D. A. Huse and M. E. Fisher, J. Phys. C 15, L585 (1982).
[40]R. J. Baxter, J. Stat. Phys. 26, 427 (1981).
[41]R. J. Baxter and P. A. Pearce, J. Phys. A 15, 897 (1982).
[42]M. E. Fisher and D. S. Fisher, Phys. Rev. B 25, 3192 (1982).
[43]H. J. Schulz, B. I. Halperin, and C. L. Henley, Phys. Rev. B 26, 3797 (1982).
[44]T. Bohr, Phys. Rev. B 25, 6981 (1982).
[45]R. Imbihl, R. J. Behm. K. Christmann, G. Ertl, and T. Matsushima, Surf. Sci. 117, 257 (1982).
[46]S. Ostlund, Phys. Rev. B 23, 2235 (1981).
[47]The wall width can be substantial: F. F. Abraham, S. W. Koch, and W. E. Rudge [Phys. Rev. Lett. 49, 1830 (1982)] simulated Kr on graphite at 97.5 K and found wall widths of approximately ten atoms.
[48]See, e.g., J. S. Rowlinson and B. Widom, *Molecular Theory of Capillarity* (Oxford University Press, London, 1982).
[49]J. V. José, L. P. Kadanoff, S. Kirkpatrick, and D. R. Nelson, Phys. Rev. B 16, 1217 (1977).
[50]See, e.g., M. E. Fisher, Proc. Nobel Symp. 24, 16 (1974), [in *Collective Properties of Physical Systems,* edited by B. Lundqvist and S. Lundqvist (Academic, New York, 1974)].
[51]M. E. Fisher, D. M. Jasnow, and M. N. Barber, Phys. Rev. A 8, 111 (1973).
[52]B. Widom, in *Phase Transitions and Critical Phenomena,* edited by C. Domb and M. S. Green (Academic, New York, 1972), Vol. 3.
[53]A. A. Migdal, Zh. Eksp. Teor. Fiz. 69, 1457 (1975) [Sov. Phys.—JETP 42, 743 (1976)].
[54]L. P. Kadanoff, Ann. Phys. (N.Y.) 100, 359 (1976).
[55]A. Aharony, J. Phys. A 10, 389 (1977).
[56]J. P. Straley and M. E. Fisher, J. Phys. A 6, 1310 (1973).
[57]R. M. Hornreich, M. Luban, and S. Shtrikman, Phys. Rev. B 19, 3799 (1979).
[58]M. Nielsen, J. Als-Nielsen, J. Bohr, and J. P. McTague, Phys. Rev. Lett. 47, 582 (1981).
[59]G. O. Williams, P. Rujan, and H. L. Frisch, Phys. Rev. B 24, 6632 (1981).
[60]J. W. Cahn, J. Chem. Phys. 66, 3667 (1977).
[61]C. Ebner and W. F. Saam, Phys. Rev. Lett. 38, 1486 (1977).
[62]D. E. Sullivan, J. Chem. Phys. 74, 2604 (1981).
[63]R. Pandit and M. Wortis, Phys. Rev. B 25, 322 (1982).
[64]R. Pandit, M. Schick, and M. Wortis, Phys. Rev. B 26, 5112 (1982).
[65]H. Nakanishi and M. E. Fisher, Phys. Rev. Lett. 49, 1565 (1982).
[66]J. Villain, in *Ordering in Strongly Fluctuating Condensed Matter Systems,* edited by T. Riste (Plenum, New York, 1980), p. 221.
[67]See, e.g., M. E. Fisher, J. Chem. Phys. 44, 616 (1965).
[68]D. B. Abraham, Phys. Rev. Lett. 44, 1165 (1980); note also D. B. Abraham and E. R. Smith, Phys. Rev. B 26, 1480 (1982).
[69]T. W. Burkhardt, J. Phys. A 14, L63 (1981).
[70]J. J. Chalker, J. Phys. A 14, 2431 (1981).
[71]S. T. Chui and J. D. Weeks, Phys. Rev. B 23, 2438 (1981).
[72]H. J. Hilhorst and J. M. J. van Leeuwen, Physica 107A, 319 (1981).
[73]See also W. Selke and D. A. Huse, Z. Phys. B 50, 113 (1983).
[74]See also (a) T. Nattermann, J. Phys. C 16, 4125 (1983), who considers quantum effects, random-field fluctuations, and long-range interactions; (b) J. Phys. (Paris) 43, 631 (1982); (c) Solid State Commun. 44, 869 (1982); (d) J. Phys. C 16, 4113 (1983).
[75]The correspondence of the present notation with that of Ref. 42 is as follows: d, l, A_l, A_0, c_d, and $\tilde{\Sigma}$ have the same meaning, but $b_{||} \equiv a_1$, $b_\perp \equiv z_0$ and the conventions adopted for $||$ and $\perp$ are opposite (since the axis *normal* to the walls was considered to be "parallel" in Ref. 42).
[76]H. J. Schulz, Phys. Rev. B 22, 5274 (1980).
[77]See, e.g., N. D. Mermin, Rev. Mod. Phys. 51, 591 (1979).
[78]Thus in the case of a junction of three superheavy *ideal* walls $A \mid B$, $B \mid C$, and $C \mid A$, as seen on the left of Fig. 3, *no defects* at all occur in the adsorbate lattice if, as usual, one constructs Voronoi polygons based on the particle positions and, in order to define a Burgers vector, chooses paths which faithfully reflect the resulting topology. The same is true of a junction of three heavy walls $B||A$, $A||C$, and $C||A$ as in the middle-left position in Fig. 3. In this case, however, the Voronoi polygons for the ideal walls shown have only five sides; however, they are structurally unstable to *shears* parallel to the walls, which will, physically, normally be induced by relaxation of the particles which enables them to increase their separation at no change in density. Such shears yield six-sided polyhedra and, again, one has no lattice defects. However, the shears impart a rotational sense, clockwise or anticlockwise, to a $(p=3)$-fold junction of heavy walls. These rotations at the walls may even act coherently in a hexagonal incommensurate phase to result in a *rotated phase* in which the axes of adsorbate lattice are skewed with respect to those of the substrate. In the absence of this, however, the shears *may* accumulate at certain places, such as the *bends* in the wall bounding the C phase in Fig. 3, resulting in 5:7 pairs of Voronoi polygons which then correspond to dislocations in the adsorbate lattice but do *not* correspond to dislocations in the order parameter sense. [See also Kardar and Berker (Ref. 6) who use the adsorbate lattice sense of dislocation.]
[79]See, e.g., C. Herring in *Structure and Properties of Solid Surfaces,* edited by R. Gomer and G. S. Smith (University of Chicago Press, Chicago, 1953).
[80]J. S. Langer and M. E. Fisher, Phys. Rev. Lett. 19, 560 (1967).
[81]See, M. E. Fisher, Physics 3, 255 (1967).
[82]R. H. Swendsen, Phys. Rev. Lett. 49, 1302 (1982).